(12) INTERNATIONAL APPLICATION PUBLISHED UNDER THE PATENT COOPERATION TREATY (PCT)

(19) World Intellectual Property Organization
International Bureau

(43) International Publication Date
3 April 2003 (03.04.2003)

PCT

(10) International Publication Number
WO 03/027961 A2

(51) International Patent Classification[7]: G06T 17/00

(21) International Application Number: PCT/US02/24220

(22) International Filing Date: 23 July 2002 (23.07.2002)

(25) Filing Language: English

(26) Publication Language: English

(30) Priority Data:
60/324,403 24 September 2001 (24.09.2001) US
10/152,444 21 May 2002 (21.05.2002) US

(71) Applicant *(for all designated States except US)*: **RAINDROP GEOMAGIC, INC.** [US/US]; 617 Davis Drive, Suite 200, Durham, NC 27713 (US).

(72) Inventors; and

(75) Inventors/Applicants *(for US only)*: **FLETCHER, G., Yates** [US/US]; 104 Bridgeway Court, Cary, NC 27511 (US). **GLOTH, Tobias** [US/US]; 1625 Discovery Way, Durham, NC 27703 (US). **EDELSBRUNNER, Herbert** [US/US]; 216 Chesley Lane, Chapel Hill, NC 27514 (US). **FU, Ping** [US/US]; 216 Chesley Lane, Chapel Hill, NC 27514 (US).

(74) Agent: **MYERS BIGEL SIBLEY & SAJOVEC**; PO Box 37428, Raleigh, NC 27627 (US).

(81) Designated States *(national)*: AE, AG, AL, AM, AT, AU, AZ, BA, BB, BG, BR, BY, BZ, CA, CH, CN, CO, CR, CU, CZ, DE, DK, DM, DZ, EC, EE, ES, FI, GB, GD, GE, GH, GM, HR, HU, ID, IL, IN, IS, JP, KE, KG, KP, KR, KZ, LC, LK, LR, LS, LT, LU, LV, MA, MD, MG, MK, MN, MW, MX, MZ, NO, NZ, OM, PH, PL, PT, RO, RU, SD, SE, SG, SI, SK, SL, TJ, TM, TN, TR, TT, TZ, UA, UG, US, UZ, VN, YU, ZA, ZM, ZW.

(84) Designated States *(regional)*: ARIPO patent (GH, GM, KE, LS, MW, MZ, SD, SL, SZ, TZ, UG, ZM, ZW), Eurasian patent (AM, AZ, BY, KG, KZ, MD, RU, TJ, TM), European patent (AT, BE, BG, CH, CY, CZ, DE, DK, EE, ES, FI, FR, GB, GR, IE, IT, LU, MC, NL, PT, SE, SK, TR), OAPI patent (BF, BJ, CF, CG, CI, CM, GA, GN, GQ, GW, ML, MR, NE, SN, TD, TG).

Published:
— *without international search report and to be republished upon receipt of that report*

For two-letter codes and other abbreviations, refer to the "Guidance Notes on Codes and Abbreviations" appearing at the beginning of each regular issue of the PCT Gazette.

WO 03/027961 A2

(54) Title: METHODS, APPARATUS AND COMPUTER PROGRAM PRODUCTS THAT RECONSTRUCT SURFACES FROM DATA POINT SETS

(57) Abstract: Methods, apparatus and computer program products provide efficient techniques for reconstructing surfaces from data point sets. These techniques include reconstructing surfaces from sets of scanned data points that have preferably undergone preprocessing operations to improve their quality by, for example, reducing noise and removing outliers. These techniques include reconstructing a dense and locally two-dimensionally distributed 3D point set (e.g., point cloud) by merging stars in two-dimensional weighted Delaunay triangulations within estimated tangent planes. The techniques include determining a plurality of stars from a plurality of points pi in a 3D point set S that at least partially describes the #D surface, by projecting the plurality of point pi onto planes Ti that are each estimated to be tangent about a respective one of the plurality of points pi. The plurality of stars are then merged into a digital model of the 3D surface.

METHODS, APPARATUS AND COMPUTER PROGRAM PRODUCTS THAT RECONSTRUCT SURFACES FROM DATA POINT SETS

Reference to Priority Application

This application claims priority to U.S. Application Serial No. 10/152,444, filed March 21, 2002 and U.S. Provisional Application Serial No. 60/324,403, filed September 24, 2001, the disclosures of which are hereby incorporated herein by reference.

Field of the Invention

This invention relates to methods and systems that reconstruct three-dimensional (3D) surfaces and, more particularly, to methods and systems that reconstruct 3D surfaces from data point sets.

Background of the Invention

Conventional techniques that use differential concepts to reconstruct surfaces from scanned data point sets typically assume a finite set of points that are sampled on the surface of a shape in a three-dimensional space and ask for an approximation of that surface. Such techniques may be classified by the assumptions they make about the data point sets. Techniques that make structural assumptions may simplify the reconstruction task by providing the points in a specific order. Techniques that make density assumptions may enable the application of differential concepts by providing sufficiently many point samples within each data point set. Techniques that avoid assumptions typically require the reconstruction operations to rely on general principles of describing geometric shapes.

One conventional technique that incorporates density assumptions is described in an article by H. Hoppe et al., entitled "Surface Reconstruction from Unorganized Points," Computer Graphics, Proceedings of SIGGRAPH, pp. 71-78 (1992). This technique uses normal estimates to generate a signed distance function from which a surface is extracted as a zero-set. Another conventional technique is described in an article by N. Amenta et al., entitled "Surface Reconstruction by Voronoi Filtering," Discrete Computer Geometry, Vol. 22, pp. 481-504 (1999). This technique exploits shape properties of three-dimensional Voronoi cells for densely sampled data points. Unfortunately, because these reconstruction techniques rely heavily on the quality of the data, they may fail if a given data point set does not adequately support the application of differential concepts. For example, these reconstruction techniques may fail if there are large gaps in the distribution of the data points in a set or if the accuracy of the data points is compromised by random noise. These techniques may also fail if the data point sets are contaminated by outliers. Data point sets having relatively large gaps, high levels of random noise and/or outliers may result from scanning objects having sharp edges and corners.

Additional surface reconstruction techniques can be distinguished based on the internal operations they perform. For example, in "sliced data" reconstruction techniques, the data points and their ordering are assumed to identify polygonal cross-sections in a finite sequence of parallel planes. This assumption may simplify the complexity of the technique, but it also typically limits the technique to data generated by a subclass of scanners. A survey of work that includes this technique is described in an article by D. Meyers et al., entitled "Surfaces from Contours," ACM Trans. on Graphics, Vol. 11, pp. 228-258 (1992). In another reconstruction technique, the data points are used to construct a map $f: \mathbb{R}^3 \rightarrow \mathbb{R}$, and the surface is constructed as the zero set, $f^{-1}(0)$. The zero set may be constructed using a marching cube algorithm that is described in an article

by W. Lorensen et al., entitled "Marching Cubes: A High Resolution 3D Surface Construction Algorithm," Computer Graphics, Proceedings of SIGGRAPH, Vol. 21, pp. 163-169 (1987). One example of this reconstruction technique is described in the aforementioned article by H. Hoppe et al. Attempts to generalize and apply surface meshing techniques to the reconstruction of surfaces from unstructured data point sets have also been presented in a survey paper by S.K. Lodha and R. Franke, entitled "Scattered Data Techniques for Surfaces," Proceedings of a Dagstuhl Seminar, Scientific Visualization Dagstuhl '97, Hagen, Nielson and Post (eds.), pp. 189-230. Additional techniques for automatically wrapping data point sets into digital models of surfaces are also disclosed in U.S. Patent No. 6,377,865 to Edelsbrunner et al., entitled "Methods of Generating Three-Dimensional Digital Models of Objects by Wrapping Point Cloud Data Points," assigned to the present assignee, the disclosure of which is hereby incorporated herein by reference.

Summary of the Invention

Methods of modeling three-dimensional (3D) surfaces include preferred techniques to reconstruct surfaces from respective sets of data points that at least partially describe the surfaces. The data points may be generated as point clouds by scanning an object in three dimensions. These reconstruction techniques may include improving the quality of the reconstructed surfaces using numerical approximations of local differential structure to reduce noise and remove outliers from the data points. The numerical approximations of local differential structure may be achieved using differential concepts that include determining surface normals at respective ones of the data points. A local differential structure of a bundle of the surface normals can be used to define principal curvatures and their directions. In particular, a number of substantially non-zero principal curvatures may be used to determine the types of approximating surfaces that can be locally fit to the data points. By construction, these approximating surfaces are typically only sensitive to an average amount of

noise that is locally present in the data points. Accordingly, the approximating surfaces vary considerably slower than the points themselves. This difference is preferably exploited in reducing the local variability of the data points and, therefore, the amount of random noise present therein. The same differential concepts may also be used to detect outliers and to subsample the data points in a curvature sensitive manner.

Methods of modeling 3D surfaces according to first embodiments of the present invention include determining an estimated normal for each of a plurality of points in a 3D data point set that at least partially describes the 3D surface. The plurality of points may constitute all or less than all of the points in the 3D point set. A differential structure of the estimated normals is evaluated to estimate principal curvature directions on the 3D surface and to classify a respective local neighborhood of each of the plurality of points in terms of its shape characteristic. An approximating surface is then determined for each of the local neighborhoods. A denoising operation may be performed on the 3D point set by moving each of the plurality of points to a respective approximating surface that is associated with a local neighborhood of the respective point. Other methods of modeling 3D surfaces may include operations to determine a respective set of near points S_i for each of a plurality of points p_i in a 3D point set S that at least partially describes the 3D surface, where $S_i \subset S$. An operation may then be performed to determine a normal bundle for the 3D point set S by determining a respective plane h_i of best fit for each of the sets of near points S_i and a respective normal n_i for each of the planes h_i of best fit. A respective approximating surface is then determined for each of the sets of near points S_i using the normal bundle to estimate respective principal curvature directions for each of the sets of near points S_i.

Methods of modeling 3D surfaces according to still further embodiments of the present invention include determining a respective set of near points for each of a plurality of points in a 3D point set that at least partially describes the 3D surface and then fitting each set of near points

with a respective approximating surface. The approximating surfaces may be selected from the group consisting of planes, cylinders and quadratic or cubic surfaces. The 3D point set is then denoised by moving each of the plurality of points in the 3D point set to the approximating surface associated with its respective set of near points. Additional embodiments include denoising a 3D point set that at least partially describes the 3D surface by classifying a first neighborhood of points in the 3D point set using (i) a mass distribution matrix (MDM) of the first neighborhood of points to estimate first normals associated with the first neighborhood of points and (ii) a normal distribution matrix (NDM) of the first normals to estimate principal curvature directions. Operations are then performed to fit an approximating surface to the first neighborhood of points and then move at least one point in the first neighborhood of points to the approximating surface to thereby reduce noise in the first neighborhood of points.

Additional methods of modeling three-dimensional (3D) surfaces include techniques to reconstruct surfaces from sets of scanned data points that have preferably undergone preprocessing operations to improve their quality by, for example, reducing noise and removing outliers as described above. These methods preferably include reconstructing a dense and locally two-dimensionally distributed 3D point set (e.g., point cloud) by merging stars in two-dimensional Delaunay triangulations within estimated tangent planes. These two-dimensional Delaunay triangulations may have vertices with non-zero weights and, therefore, may be described as weighted Delaunay triangulations. In particular, these methods include determining a plurality of stars from a plurality of points p_i in a 3D point set S that at least partially describes the 3D surface, by projecting the plurality of points p_i onto planes T_i that are each estimated to be tangent about a respective one of the plurality of points p_i. The plurality of stars are then merged into a digital model of the 3D surface.

The operations to determine a plurality of stars preferably include identifying a respective subset of near points S_i for each of the plurality of points p_i and projecting a plurality of points p_j in each subset of near points S_i to a respective estimated tangent plane T_i. In particular, for each of a plurality of estimated tangent planes, T_i, a star of the projection of a respective point p_i onto the estimated tangent plane T_i is determined. The star of the projection of a respective point p_i onto the estimated tangent plane T_i constitutes a two-dimensional (2D) Delaunay triangulation (e.g., 2D weighted Delaunay triangulation). To improve efficiency, the operation to identify a respective subset of near points S_i for each of the plurality of points p_i may include storing the 3D point set S in an oct-tree. This operation may also include determining a width $2r_0$ of a near point search cube using a random sample $R \subset S$, where r_0 is a positive real number. Then, for each of the plurality of points p_i, a subset of k_0 points that are closest in Euclidean distance to p_i may be determined, where k_0 is a positive integer. From this subset, all closest points that are also within a respective near point search cube, which is centered about a corresponding point p_i and has a width equal to $2r_0$, are selected.

Additional techniques to reconstruct surfaces include modeling a three-dimensional (3D) surface by determining a plurality of stars from a plurality of points p_i in a 3D point set S that at least partially describes the 3D surface, by projecting each of the plurality of points p_i onto a respective plane T_i that is estimated to be tangent about the corresponding point p_i. Weights, which are based on projection distance (e.g., (projection distance)^2), are also preferably assigned to each projected point so that subsequent operations to merge triangles and edges result in fewer conflicts and, therefore, fewer holes in resulting digital models. The plurality of stars are then merged into a model of the 3D surface. The merging operation includes eliminating edges and triangles from the plurality of stars that are in conflict and merging nonconflicting edges and triangles into a surface triangulation. The merging operation may include

sorting triangles within the plurality of stars and removing those sorted triangles that are not in triplicate. The sorted triangles that have not be removed are then connected to define a triangulated pseudomanifold as a two-dimensional simplicial complex in which edges and triangles of a star that share a vertex form a portion of an open disk. Operations may also be performed to sort edges within the plurality of stars that do not belong to any of the triangles in the triangulated pseudomanifold and remove those sorted edges that are not in duplicate. The sorted edges that have not been removed may then be added to the triangulated pseudomanifold.

Still further methods include improving the quality of a scanned data point set by removing noise and/or eliminating outliers therefrom and/or subsampling the point set, and then reconstructing a surface from the improved data point set. These methods preferably include determining a respective set of near points S_i for each of a first plurality of points $p1_i$ in a first 3D point set $S1$ that at least partially describes the 3D surface, where $S_i \subset S1$. Each set of near points S_i is fit with a respective approximating surface. A denoising operation is then performed which converts the first 3D point set $S1$ into a second 3D point set $S2$. This denoising operation is performed by moving at least some of the first plurality of points $p1_i$ in the first 3D point set $S1$ to the approximating surfaces associated with their respective sets of near points S_i. Although rare, if the operation to move a point to a respective approximating surface requires a spatial translation that exceeds a designated threshold value, then the point may be removed as an outlier. A plurality of stars are then determined from a second plurality of points $p2_i$ in the second 3D point set $S2$. These stars are determined by projecting the second plurality of points $p2_i$ onto planes T_i that are estimated to be tangent about a respective one of the second plurality of points $p2_i$. The stars are then merged into a digital model of the 3D surface.

The operations to fit each set of near points S_i with a respective approximating surface comprise fitting a first set of near points S_1 with a

first approximating surface by determining respective planes h_i of best fit for each of a plurality of points p_i in the first set of near points S_r and then determining an estimated normal n_j for each of the points p_i as a normal of its respective plane h_i of best fit. A shape characteristic of the first set of near points S_r is also classified by determining estimates of principal curvature directions for a point $p1_i$ from a plurality of the estimated normals n_j. The shape characteristic may be plane-like and/or edge-like and/or corner-like.

According to still further preferred aspects of these embodiments, the operations to determine a plurality of stars include operations to determine weighted Delaunay triangulations on tangent planes. In particular, these operations may include determining a star of a first point in a 3D point set that at least partially describes the 3D surface, by: (i) projecting the first point and at least second, third and fourth points in a neighborhood of the first point in the 3D point set to a plane, (ii) assigning respective weights to each of the second, third and fourth points that are based on projection distance, and (iii) evaluating whether the projection of the fourth point is closer than orthogonal to an orthocenter of a first triangle having projections of the first, second and third points as vertices. If the projection of the fourth point is closer than orthogonal, then it is included as a vertex of a new triangle in the star of the projection of the first point and the first triangle is discarded. If the projection of the fourth point is farther than orthogonal, then it is included as a vertex of a new triangle containing the first, third and fourth points as vertices.

Additional embodiments of the present invention may also include operations to create stars of projected points by sequentially connecting a neighborhood of projected points on a plane to a first projected point on the plane by evaluating whether at least one projected point in the neighborhood of projected points is closer than orthogonal to an orthocenter of an orthocircle. This orthocircle is defined by a triangle containing the first projected point and two projected points in the

neighborhood of projected points as vertices, with the neighborhood of projected points having weights associated therewith. These weights are each a function of a projection distance between a respective projected point in the neighborhood of projected points and a corresponding point in a 3D point set that at least partially describes the 3D surface.

Still further operations may include projecting a first point in a 3D point set that at least partially describes the surface and a set of points in a neighborhood of the first point to a plane that is estimated to be tangent to the surface at the first point. An operation may then be performed to create a weighted Delaunay triangulation comprising triangles that share a projection of the first point in the plane as a vertex and include at least some of the projections of the set of points in the neighborhood of the first point as vertices that are weighted as a function projection distance squared.

Embodiments of the present invention may also include operations to model a three-dimensional (3D) surface by projecting a first point in a 3D point set that at least partially describes the surface and a set of points in a neighborhood of the first point to a plane that is estimated to be tangent to the surface at the first point. Additional operations include creating a weighted Delaunay triangulation comprising triangles that share a projection of the first point in the plane as a vertex and include at least some of the projections of the set of points in the neighborhood of the first point as vertices that are weighted as a function of projection distance. Operations to create a weighted Delaunay triangulation may include operations to evaluate whether or not one or more of the projections of the set of points in the neighborhood of the first point are closer than orthogonal to an orthocenter of a first triangle in the weighted Delaunay triangulation. The operations to create a weighted Delaunay triangulation may include evaluating a 4x4 matrix containing coordinates of the vertices of the first triangle as entries therein along with entries that are functionally dependent on the weights associated with the vertices of the first triangle.

These operations to evaluate the matrix may include computing a determinant of the matrix.

Brief Description of the Drawings

FIG. 1 illustrates a closed axis-aligned cube that may be used when determining collections of near points.

FIG. 2 illustrates a standard triangle $A_1A_2A_3$ with shading that corresponds to data point sets that are strongly corner-like, edge-like and plane-like.

FIG. 3 illustrates construction of an oct-tree in two dimensions.

FIG. 4 illustrates shaded stars within a weighted Delaunay triangulation.

FIG. 5 illustrates sequential operations to construct a star.

FIG. 6 illustrates a trist data structure comprising an array of (unordered) triangles connected to each other by adjacency.

FIG. 7 illustrates five dummy triangles, four of which connect ω to boundary edges and one of which connects ω to a principal edge in a star of p_i.

FIG. 8 illustrates two 'crossing' principal edges and two 'crossing' triangles.

FIG. 9 illustrates a hole whose cycle of seven directed edges includes two along a principal edge of a pseudomanifold.

FIG. 10 illustrates an embedding of a directed boundary cycle that cuts a plane into an open disk on its left and one or more shaded open regions on its rights.

FIG. 11 illustrates a set of points, including p_1 and p_2, that define a portion of a three-dimensional (3D) surface.

FIGS. 12A-12D are illustrations that describe operations to create stars by sequentially connecting points projected to respective tangent planes and generate stars, according to embodiments of the present invention.

FIG. 13 illustrates a 3D triangulation that results from merging the stars illustrated by FIG. 12D.

FIGS. 14A-14G illustrate operations to sequentially connect projected points according to embodiments of the present invention.

FIG. 15 is a flow-diagram that illustrates operations for modeling three-dimensional surfaces according to embodiments of the present invention.

FIG. 16 is a flow-diagram that illustrates operations for modeling three-dimensional surfaces according to embodiments of the present invention.

FIG. 17 is a flow-diagram that illustrates preferred operations for merging stars according to embodiments of the present invention.

FIG. 18 is a flow-diagram that illustrates operations for preprocessing three-dimensional point sets to reduce noise, according to embodiments of the present invention.

FIG. 19 is a flow-diagram that illustrates operations for preprocessing three-dimensional point sets to reduce noise, according to embodiments of the present invention.

FIG. 20 is a flow-diagram that illustrates operations for modeling three-dimensional surfaces according to embodiments of the present invention.

FIG. 21 is a block diagram that illustrates a general hardware description of a computer workstation that performs operations according to embodiments of the present invention.

Description of a Preferred Embodiment

The present invention now will be described more fully hereinafter with reference to the accompanying drawings, in which preferred embodiments of the invention are shown. This invention may, however, be embodied in many different forms and applied to other articles and should not be construed as limited to the embodiments set forth herein; rather, these embodiments are provided so that this disclosure will be thorough and complete, and will fully convey the scope of the invention to those skilled in the art. The operations of the present invention, as described more fully hereinbelow and in the accompanying figures, may be performed by an entirely hardware embodiment or, more preferably, by an embodiment combining both software and hardware aspects and some degree of user input. Furthermore, aspects of the present invention may take the form of a computer program product on a computer-readable storage medium having computer-readable program code embodied in the medium. Any suitable computer-readable medium may be utilized including hard disks, CD-ROMs or other optical or magnetic storage devices. Like numbers refer to like elements throughout.

Various aspects of the present invention are illustrated in detail in the following figures, including flowchart illustrations. It will be understood that each of a plurality of blocks of the flowchart illustrations, and combinations of blocks in the flowchart illustrations, can be implemented by computer program instructions. These computer program instructions may be provided to a processor or other programmable data processing apparatus to produce a machine, such that the instructions which execute on the processor or other programmable data processing apparatus create means for implementing the operations specified in the flowchart block or blocks. These computer program instructions may also be stored in a computer-readable memory that can direct a processor or other programmable data processing apparatus to function in a particular manner, such that the instructions stored in the computer-readable memory

produce an article of manufacture including instruction means which implement the operations specified in the flowchart block or blocks.

Accordingly, blocks of the flowchart illustrations support combinations of means for performing the specified operations, combinations of steps for performing the specified operations and program instruction means for performing the specified operations. It will also be understood that each of a plurality of blocks of the flowchart illustrations, and combinations of blocks in the flowchart illustrations, can be implemented by special purpose hardware-based computer systems that perform the specified operations or steps, or by combinations of special purpose hardware and computer instructions.

Methods of modeling three-dimensional (3D) surfaces according to embodiments of the present invention include preferred techniques to reconstruct a surface from data points that at least partially describe the surface. The data points may be generated as point clouds by scanning an object in three dimensions. These reconstruction techniques may include operations to improve the quality of the reconstructed surfaces using numerical approximations of local differential structure to reduce noise and remove outliers from the data points. The numerical approximations of local differential structure may be achieved using differential concepts that include determining surface normals at respective ones of the data points. A local differential structure of a bundle of the surface normals can be used to define principal curvatures and their directions. In particular, a number of substantially non-zero principal curvatures may be used to determine the types of approximating surfaces that can be locally fit to the data points. By construction, these approximating surfaces are typically only sensitive to an average amount of noise that is locally present in the data points. Accordingly, the approximating surfaces vary considerably slower than the points themselves. This difference is preferably exploited in reducing the local variability of the data points and, therefore, the amount of random noise present therein. The same differential concepts may also be used to

detect outliers and to subsample the data points in a curvature sensitive manner.

The numerical approximations of local differential structure are preferably obtained using mean square error minimization techniques. A mass distribution matrix (MDM) of a local collection of data points is used to estimate normals and a normal distribution matrix (NDM) of a local collection of normals is used to estimate principal curvature directions. In both cases, a preferred numerical method includes the spectral decomposition of the matrix, which provides direction estimates through eigenvectors and variability estimates through eigenvalues. Numerical stability can be improved by normalizing all input data and by using standard operations for the singular value decomposition of the matrices. Because a time consuming operation includes finding a set of near points for each of a plurality of points in the data point set, an implict oct-tree is used to store the data point set in an efficient manner.

In particular, operations to improve the quality of surfaces generated by surface reconstruction techniques include identifying collections S_i for each of a plurality points p_i (and possibly all points) in a finite three-dimensional (3D) set S of points that are relatively densely distributed on a surface in $\mathbb{R}^3$, where $S_i \subset S$ and $p_i \in S_i$. Each collection S_i is referred to herein as the set of "near points" of p_i and is used as a primary source of information about the neighborhood of p_i on the surface. In particular, S_i is the collection of points $p_j \in S$ that lie within a closed and axis-aligned cube **10** that has a side-length of $2r_0$ and is centered at p_i. This is illustrated by FIG. 1, where the solid black points located within the cube **10** belong to S_i. The real number constant r_0 is chosen such that an expected size of the sets of near points S_i is some constant yield, which may be a user-defined integer. Typical values for low, medium and high yield are 25, 50 and 100, respectively. As described more fully hereinbelow, to compute a set of near points S_i for each of a plurality of points p_i, the data point set $S \subset \mathbb{R}^3$ is stored in an implicit oct-tree. A random sample $R \subset S$ is used to compute a width

$2r_0$ of a closed and axis-aligned cube **10** having a specified (e.g., user specified) average yield. Then, for each point $p_i \in S$, a subset of k_0 nearest points is computed. Those points in the subset that also lie within the cube of width $2r_0$ (centered at p_i) are then selected as points in a respective near point set S_i. The validity of the operations described herein are independent of the value of the specified average yield, but the value of the yield influences the results they generate and the computing time required to generate the results.

For a given set of near points S_i corresponding to a point $p_i \in S$, the plane that minimizes a mean square distance to the near points necessarily passes through the centroid of the points. The near points may be translated by minus the centroid or, equivalently, the centroid can be treated as the origin and only planes of zero offset relative to the origin need be considered. Each such plane can be written as the set of points $x \in \mathbb{R}^3$ that satisfy the relationship $x^T u=0$ for some unit normal $u \in S^2$. The sum of the square distances of the points $p_j \in S_i$ from a plane having zero offset is:

$$E_i(u) = \sum_j (p_j^T u)^2$$

$$= u^T \left(\sum_j p_j p_j^T \right) u$$

The mass distribution matrix $\mathbf{M}_i = \sum p_j p_j^T$ is symmetric and positive semi-definite and thus has three non-negative real eigenvalues $\mu_1 \geq \mu_2 \geq \mu_3$. Accordingly, $\mathbf{M}_i = U \Delta U^T$, where:

$$\Delta = \begin{bmatrix} \mu_1 & 0 & 0 \\ 0 & \mu_2 & 0 \\ 0 & 0 & \mu_3 \end{bmatrix}$$

The columns of U are the corresponding unit eigenvectors e_1, e_2 and e_3 in the same order. Multiplication with U^T puts a point p_i into the coordinate frame spanned by the eigenvectors, and multiplication with U puts it back into the original coordinate frame. For a direction $u = u_1e_1 + u_2e_2 + u_3e_3$, the sum of square distance is $E_i(u) = \mu_1(u_1^2) + \mu_2(u_2^2) + \mu_3(u_3^2)$. The preimage of unity is the ellipsoid $E_i^{-1}(1)$, and the half-axes of $E_i^{-1}(1)$ have lengths equal to $(\mu_i)^{-\frac{1}{2}}$ along u_i. The unit vector with smallest error is therefore in the direction of the longest half-axis, which is parallel to e_3. The plane of best fit, h_i, therefore consists of the points x that satisfy $x^Te_3 = 0$. The plane of best fit, h_i, typically does not pass through p_i. The unit normal n_i to the plane of best fit h_i is treated herein as the estimated normal at p_i. To improve run time for situations involving three-by-three matrices, which are the most common, the eigenvalues are computed as the roots of the characteristic polynomial. The first root is approximated by Newton iteration, and the other two by solving the remaining quadratic equation analytically. Other techniques for computing eigenvalues may also be used.

The estimated normals n_i at the points p_i are used to estimate principal curvature directions on the surface (i.e., two principal curvature directions for each point p_i). These estimates of principal curvature directions are then used to classify the local neighborhood of each point p_i in terms of its shape characteristics. In particular, the function $F_i: \mathbb{R}^3 \rightarrow \mathbb{R}$ is used that sums the square distances to the normal planes passing through the origin, which is defined by:

$$F_i(x) = \sum_{p_j \in S_i} (x^T n_j)^2$$

$$= x^T \left(\sum_{p_j \in S_i} n_j n_j^T \right) x .$$

Similar to the mass distribution matrix M_i, the normal distribution matrix N_i = $= \sum n_j n_j^T$ is symmetric and positive semi-definite with non-negative eigenvalues $v_1 \geq v_2 \geq v_3$. A large eigenvalue corresponds to a direction in which the sum of squared scalar products or, equivalently, the sum of square distances to the normal planes increases quickly. Accordingly, a set of near points S_i can be treated as having plane-like configuration if there is only one such principal curvature direction or, equivalently, only one large eigenvalue.

Operations to classify a local neighborhood of each point p_i in terms of its shape characteristics continue by normalizing the eigenvalues to $t_l = (v_l)(v_1 + v_2 + v_3)^{-1}$, for l = 1, 2 and 3, where $t_1 + t_2 + t_3 = 1$ and $t_1 \geq t_2 \geq t_3$. As illustrated by FIG. 2, the triplets of numbers t_l that satisfy these conditions define a triangle in a barycentric subdivision of a standard triangle. The smaller two eigenvalues correspond to the two principal curvatures. Neighborhoods with two, one and zero substantially non-zero principal curvatures are classified using two constants ϵ_0, ϵ_1 that meet the following relationship: $0 < \epsilon_0 < \epsilon_1 < 1/3$. The shape classification thresholds ϵ_0 and ϵ_1 may be set at 0.0075 and 0.015, respectively. A set of near points S_i is treated as strongly plane-like, edge-like or corner-like based on the following relationships:

$$\text{plane-like} \rightarrow \epsilon_0 \geq t_2 \geq t_3$$
$$\text{edge-like} \rightarrow \epsilon_0 \geq t_3 \text{ and } \epsilon_1 \leq t_2$$
$$\text{corner-like} \rightarrow \epsilon_1 \leq t_3 \leq t_2.$$

Similarly, a set of near points S_i is treated as being weakly plane-like, weakly edge-like and weakly corner-like if the normalized eigenvalues satisfy the same inequalities with ϵ_0 and ϵ_1 interchanged. As illustrated by FIG. 2, the points $t_1A_1 + t_2A_2 + t_3A_3$ populate the lower left triangle in the

barycentric subdivision of the standard triangle $A_1A_2A_3$ **20**. The light, medium and dark shaded areas correspond to data point sets that are strongly corner-like, strongly edge-like and strongly plane-like, respectively. The white strips between the shaded areas correspond to data point sets that have at least two weak classifications. FIG. 2 also illustrates that each set of near points S_i has at most one strong classifier, and if it has no strong classifiers then it has at least two weak classifiers. More precisely, the region of multiple weak classifications overlaps the region of strong classifications only along a boundary. The normalized eigenvalues can therefore be used to express each multiple weak classification as a linear combination of strong classifications.

The normalized eigenvalue s_i equals $(t_i - \epsilon_0)/(\epsilon_1 - \epsilon_0)$, provided that $\epsilon_0 \le t_i \le \epsilon_1$, and this is the solution to the linear interpolation $t_i = (1- s_i)\epsilon_0 + s_i\epsilon_1$ between ϵ_0 and ϵ_1. The normalized eigenvalues s_2 and s_3 are used to linearly interpolate between strong classifications. For Case 1, where $t_3 < \epsilon_0 \le t_2 \le \epsilon_1$, the set of near points S_i is both weakly plane-like and weakly edge-like, but not weakly corner-like. The normalized eigenvalue s_2 is defined, and for S_i the fraction $1-s_2$ is considered strongly plane-like and the fraction s_2 is considered strongly edge-like. For Case 2, where $\epsilon_0 \le t_3 \le t_2 \le \epsilon_1$, the set of near points S_i has all three weak classifications. For the set of near points S_i, the fraction $1-s_2-s_3$ is considered plane-like, the fraction s_2 is considered edge-like and the fraction s_3 is considered corner-like. For Case 3, where $\epsilon_0 < t_3 < \epsilon_1 < t_2$, the set of near points S_i is both weakly edge-like and weakly corner-like, but not weakly plane-like. For the set of near points S_i, the fraction $1-s_3$ is considered strongly edge-like and the fraction s_3 is considered strongly corner-like.

In regions of low curvature, the local surface can be approximated by a plane and the plane of best fit h_i can be determined directly from the mass distribution matrix (MDM). In regions of non-trivial curvature, the local shape can be approximated by surfaces that are more complicated than planes. Cylinders with conic cross-sections can be used for near point sets

S_i that are edge-like and paraboloids can be used for near point sets S_i that are corner-like.

The set of near points S_i is edge-like if the normals lie roughly along a great-circle of the sphere of directions. The best approximation of the direction normal to that great-circle is the eigenvector that corresponds to the smallest eigenvalue of the normal distribution matrix (NDM). This is an approximation of the minor principal curvature direction, which will be referred to herein as a fold direction. The local shape can be approximated by a cylinder constructed by sweeping a line parallel to the fold direction along a conic in the orthogonal plane. Let g_i be this plane passing through p_i, and let S_i' consist of the points in S_i projected along the fold direction onto g_i. The conic g_i is constructed by least square optimization. The family of conics considered are the zero-sets of the functions G_i: $\mathbb{R}^2 \to \mathbb{R}$ defined by:

$$G_i(x) = a_1x_1^2 + a_2x_1x_2 + a_3x_2^2 + a_4x_1 + a_5x_2 + a_6,$$

where x_1 and x_2 are the coordinates in g_i measured along the other two eigenvector directions, using p_i as the origin. The family of conics contains pairs of intersecting lines as limits of progressively narrower hyperbolas. These intersecting lines are important because they model common sharp edges on the surface. Multiplying the entire polynomial by a constant does not change the zero-set, so the assumption that $\sum a_i = 1$ can be used. The function G_i may be treated as an affine function $\mathbb{R}^5 \to \mathbb{R}$ that takes a point in homogeneous coordinates, $x^T = (x_1^2, x_1x_2, x_2^2, x_1, x_2, 1)$, to the residual, $G_i(x)$. Each point $p_j' \in S_i'$ defines such a point $x_j \in \mathbb{R}^5$. The affine function that minimizes a sum of the squared residuals is:

$$\sum_j G_i(x_j)^2 = \sum_j (x_j^T a)^2$$

$$= a^T \left(\sum_j x_j x_j^T \right) a \ ,$$

where $a^T = (a_1, a_2, a_3, a_4, a_5, a_6)$. The six-by-six matrix $X_i = \sum x_j x_j^T$ is again symmetric and positive semi-definite and thus has six non-negative real eigenvalues. The affine function of best fit is determined by the unit eigenvector a that corresponds to the smallest of the six eigenvalues.

When the matrix X_i, which is computed for an edge-like neighborhood, has two almost equally small eigenvalues, then the conic of best fit may be ambiguous. In this case, a preferred operation considers both corresponding conics and projects the point to the closest of the points computed for both conics.

The sets of near points S_i that are corner-like permit the largest amount of variation and, therefore, are typically the most difficult to locally approximate. Ideally, a family of surfaces that contains triplets of intersecting planes is used. The family of zero-sets of cubic polynomials in three variables contains such triplets but leads to linear systems with as many as twenty unknowns. Contrasting this with the fact that points with corner-like neighborhoods are naturally the least common in surfaces bounding physical artifacts, an option is pursued that allows a solution of a significantly smaller optimization problem. The specific problem is finding the optimum function in the family of functions G_i defined above. The coordinate frame, within which the functions G_i are considered, consist of the three unit eigenvectors of the normal distribution matrix (NDM). Specifically, x_3 is measured in the surface normal direction, which is approximated by the eigenvector that corresponds to v_1, and x_1, x_2 are measured in the other two eigenvector directions.

The minimization problem is different from the above because the graph of G_i, and not the zero-set of G_i, is of interest. G_i is again interpreted as an affine function $\mathbb{R}^5 \to \mathbb{R}$. For each $p_j \in S_i$, x_j is defined as described above and z_j is treated as the x_3-coordinate of p_j within the frame of eigenvectors. The new residual is $G_i(x_j) - z_j$ and the sum of squared residuals is computed as:

$$H_i(a) = \sum_j (G_i(x_j) - z_j)^2$$

$$= a^T X_i a - 2a^T y_i + \sum_j z_j^2$$

where: $$y_i = \sum_j z_j x_j .$$

To compute the minimum a, all partial derivatives are set to zero. This yields:

$$\frac{\partial H_i(a)}{\partial a_l} = \frac{\partial a^T}{\partial a_l} X_i a + a^T X_i \frac{\partial a}{\partial a_l} - 2\frac{\partial a^T}{\partial a_l} y_i$$

$$= X_{il}^T a + a^T X_{il} - 2y_{il},$$

for $1 \le l \le 6$, where X_{il} is the lth column of X_i and y_{il} is the lth entry in y_i. Thus, the minimum a is the solution to the linear system $X_i a = y_i$. This system can be treated as well-conditioned.

The purpose of computing the approximating surfaces is to improve the quality of the description of the surface defined by the data point set. The primary goals are to reduce noise and remove outliers. The type of noise that is typically reduced is manifested by points that are close to but extend slightly above or below the surface. It is a common phenomenon in scanned data and can be caused by a variety of shortcomings of the scanning hardware. The approach to reduce noise is based on the observation that the approximating surface varies only slightly for nearby points, simply because it is computed from sets of near points S_i that are largely the same. Noise is preferably reduced by moving each point p_i onto the approximating surface computed for S_i. Three cases are distinguished as follows.

In the first case, S_i is plane-like. The approximating surface is the plane of best fit h_i with normal vector n_i. By construction, the centroid of S_i

lies on this plane. The point p_i is moved to its orthogonal projection on h_i. The orthogonal projection of the point is p_i'', where:

$$p_i'' = p_i - ((p_i - \bar{p}_i)^T n_i) n_i ,$$

and the centroid is represented as $\bar{p}_i$. The point p_i'' may also be referred to as the de-noised location of p_i'.

In the second case, S_i is edge-like. The surface is a cylinder whose cross-section in g_i is the conic of best fit, $G_i^{-1}(0)$. The gradient of G_i at a point $x \in g_i$ is:

$$\nabla G_i(x) = \begin{bmatrix} 2a_1x_1 + a_2x_2 + a_4 \\ a_2x_1 + 2a_3x_2 + a_5 \end{bmatrix}.$$

By construction, p_i lies at the origin of g_i, which implies that the gradient at p_i is:

$$\nabla G_i(0) = [a_4, a_5]^T ,$$

The point p_i can be moved iteratively in small steps along the gradient. Since p_i is mostly already very close to the conic, this iterative procedure is simplified and the point p_i is moved in one step. Formally, the projection of p_i is computed as:

$$p_i'' = t[a_4, a_5]^T ,$$

such that:

$$G_i(p_i'') = t^2(a_1a_4^2 + a_2a_4a_5 + a_3a_5^2) + t(a_4^2 + a_5^2) + a_6$$

vanishes. Both roots of this quadratic polynomial are computed, and the point p_i'' that is closest to point p_i is selected.

In the third case, S_i is corner-like. The approximating surface is the graph of the quadratic function G_i of best fit. The point p_i is projected in the x_3-direction onto that graph. By construction, p_i is the origin of the

coordinate system, so $p_i''=(0,0,G_i(0))$, again expressed in the local coordinate frame spanned by the eigenvectors of the normal distribution matrix. For strongly classified sets S_i, the point p_i'' is substituted for p_i. For sets S_i with mixed weak classifications, two or three points p_i'' are computed and the linear combination is substituted for p_i. In each case, the point p_i'' is dropped from the computations if the fit of the surface is not sufficiently tight, or more specifically, if the normalized smallest eigenvalue exceeds some constant δ_0. Such cases are unlikely for plane-like and edge-like sets, because the surfaces typically fit well to the data points, but they are relatively more common for corner-like sets. Corner-like neighborhoods may be better approximated by implicit cubic polynomials, which include triplets of planes in their family. Many cases occurring in practice could also be improved by approximations within certain sub-families of surfaces, such as intersections of planes with circular cylinders or cones.

Outliers are points that are far from the surface and may be created either by mistake or by physical shortcomings of the scanning hardware. Outliers may cause trouble in the reconstruction of the surface and are preferably removed before they do so. Because the surface is not known, outliers can be detected only with indirect methods. A straightforward approach for detecting outliers specifies a threshold and removes points whose square distances to the planes of best fit exceed that threshold. A drawback of this method is that many or all points with edge-like and corner-like neighborhoods are likely to be classified as outliers. This method is refined by observing that points in such edge or corner regions have near points with similarly large square distances to their planes of best fit. To discriminate between points with and without such near points, the average square distance between points and corresponding planes of best fit are considered. This average is:

$$\bar{D}=\frac{1}{n}\sum_i ((p_i-\bar{p}_i)^T n_i)^2.$$

The point p_i is treated as an outlier if its square distance exceeds a constant times the average as expressed by:

$$(p_i^T n_i)^2 > C_0 \overline{D}.$$

After computing all square distances, the outliers are identified by evaluating this simple inequality. It can easily be modified by adjusting the constant C_0. The above-described operations may be treated as preprocessing operations that reduce noise and remove outliers from the data points so that the quality of surfaces reconstructed therefrom can be improved.

Operations to reconstruct three-dimensional (3D) surfaces from dense and locally two-dimensionally distributed data points sets (e.g., point clouds) will now be described. As described above, these data point sets preferably undergo preprocessing operations to reduce noise and remove outliers, before reconstruction operations are performed. These reconstruction operations include generating a plurality of stars by locally projecting sampled points within a point set onto estimated tangent planes and then merging the stars in two-dimensional Delaunay triangulations within the estimated tangent planes. The Delaunay triangulations are preferably constructed as weighted Delaunay triangulations, however, Delaunay triangulations having unweighted vertices may also be constructed if less accurate results or less efficient operations are acceptable. The reconstruction operations return a two-dimensional simplicial complex in which the edges and triangles that share a vertex form a portion of an open disk. Such complexes are treated herein as pseudomanifolds.

Although the surface reconstruction operations described herein are based on concepts from differential geometry, they may be classified as surface meshing operations. The reconstruction operations may be arranged in four stages, and rely on the data point set $S \subset \mathbb{R}^3$ being densely sampled on the surface of an object or otherwise densely generated. These four stages include:

(A) Finding, for each of a plurality points $p_i \in S$, a respective subset of near points $S_i \subseteq S$, which contains p_i;

(B) Estimating a tangent plane using S_i, projecting S_i onto that plane, and constructing the star of p_i in the two-dimensional Delaunay triangulation;

(C) Eliminating edges and triangles that do not belong to the stars of all their vertices, and constructing the surface from what remains; and

(D) Performing post-processing by identifying and filling holes in the surface created by the elimination of edges and triangles during stage C.

As described above with respect to FIG. 1, the operations of stage A, which include searching for and identifying a respective set of near points S_i for each of a plurality of points p_i, can be time-consuming. To improve the efficiency of determining a respective set of near points S_i for each of a plurality of points p_i, a data structure that exploits the locality of the access is used for repeated searching. The near point search operations include storing an input set $S \subseteq \mathbb{R}^3$ in an implicit oct-tree and then using a random sample $R \subseteq S$ to compute a width $2r_0$ of cubes having a specified average yield m_0. For each point $p_i \in S$, a subset of k_0 nearest points that lie in the cube of width $2r_0$, centered at p_i, is computed. To describe this in mathematical terms, the box function $\square_i(r)$ is defined as the set of points $p_j \in S$ with an l_∞-distance at most r from point p_i, where r is a real number. Stated alternatively, the box function defines a set of points p_j that are contained within the closed axis-aligned cube of width $2r$ centered at p_i. Now using the Euclidean distance, we define $N_i(k)$ as the set of k points closest to p_i, including p_i itself. The set of near points of p_i is then:

$$S_i = \square_i(r_0) \cap N_i(k_0),$$

where r_0 is the positive real number computed to achieve a specified average yield and k_0 is a positive integer constant. It makes sense to define

k_0 a few times the average degree of a vertex in a flat triangulation, which is about six. In a typical case, $k_0 = 30$.

Operations for constructing an oct-tree will now be described. Additional information relating to the construction of oct-trees can be found in a two-volume textbook by H. Samat, entitled Spatial Data Structures: Quadtrees, Octrees, and Other Heirarchical Methods, Addison-Wesley (1989). Upon normalization, the input data point set can be treated as being contained in a half-open unit cube, $S \subset [0, 1)^3$. The oct-tree corresponds to a recursive decomposition of this half-open cube into eight congruent half-open cubes. FIG. 3 illustrates the construction of an oct-tree **30** in two dimensions, where a square **32** is recursively decomposed into four smaller squares. Each node μ of the oct-tree **30** is assigned an integer address that encodes the path from the root to μ. Three bits per level are required in the illustrated example, which allows at most $l_0 = 10$ levels in order to fit each address into a 32 bit word. The oct-tree is constructed from top down, with each node being decomposed as long as its level is less than l_0 and the number of points in its half-open cube exceeds $n_0 = 30$.

A leaf is a node that is not decomposed any further. The oct-tree is represented by its pre-order sequence of leaves and a parallel sequence of points. The ordering provides that the points that lie inside a cube of a node are contiguous in the second sequence. Each leaf stores its address and the index interval of the points in its cube. Navigation is done through bit manipulations of node addresses. The problem of enumerating all points inside a cube C will now be considered as an example. Let $C(\mu)$ be the half-open cube of node μ, let $S(\mu) = S \cap C(\mu)$, and write ρ for the root of the oct-tree. The points in C can be found by calling function POINTS with $\mu = \rho$, as illustrated by the following program code:

```
void POINTS (C, μ)
    if C(μ) ⊆ C then return S(μ) endif;
    if C(μ) ∩ C ≠ 0 then
      if μ is a leaf then return S(μ) ∩ C endif;
```

forall children v of μ do POINTS (C, v) endfor
endif.

The next operation includes computing a distance r_0 that is small enough (but not too small) to estimate differential properties of the surface. Two empirically tested constants $m_0 = 100$ and $s_0 = 100$ can be used, where m_0 represents a desired average yield that may be selected by a user and s_0 represents the size of the random sample $R \subseteq S$.

The yield of an axis-aligned cube is defined as the number of points of S it contains. For a given real number $r > 0$, the average yield is computed from all axis-aligned cubes of width $2r$ centered at points in S. The real number r_0 is defined as the smallest value of r for which the average yield is at least m_0. Computing this value of r is typically time-consuming, but it can be estimated quickly by choosing a random sample $R \subseteq S$ of size s_0, and computing the average yield $m(r)$ over the cubes centered at points in R. The real number r_0 is computed as the minimum value of r for which $m(r) \geq m_0$. To save time, a small estimate is used as a start and then it is improved by first growing and then by shrinking the interval, as illustrated by the following program code:

$a = 0.0$; $b = 0.001$;
while $m(b) < m_0$ do $b = 2b$ endwhile;
for $i = 1$ to l_0 do $x = (a + b)/2$;
if $m(x) < m_0$ then $a = x$ else $b = x$ endif
endfor.

After completing the iteration, $r_0 = b$ can be used, which may be a little larger than promised, or r_0 can be selected as the $s_0 m_0$ smallest distance defined by the points in the sets $\square_i(b)$, over all $p_i \in R$. Important operations include (i) computing $m(r)$ and (ii) selecting from a set of distances. The former uses function POINTS illustrated above and the

latter is performed using a one-sided version of randomized quicksort, which is described more fully hereinbelow.

Operations to compute the sets S_i of near points, for all $p_i \in S$ will now be described. These operations may be the same as those used to determine the width of the near point search cube, but speed is more critical because the operations to compute sets of near points are applied to more points. The value C_i is written for the axis-aligned cube of width $2r_0$ with center p_i and ρ for the root of the oct-tree, as illustrated by the following program code:

```
for i = 1 to n do
    N = POINTS(C_i, ρ);
    select S_i as subset of k_0 points in N closest to p_i
endfor.
```

A one-sided version of randomized quicksort is used to select points. To understand this operation, suppose N is a linear array storing the points in an arbitrary order. Quicksort splits the array using a randomly chosen pivot point, p. Specifically, function SPLIT rearranges the array so that the points to the left of p are closer to p_i and the points to the right of p are farther from p_i. The function then returns the position of the pivot. Instead of recursively sorting on both sides of that position, the recursive sort is performed only on one side. Initially, lo and hi are the first and last indices in N and $k = k_0$. These operations are illustrated by the following program code:

```
integer SELECT (k, lo, hi)
    assert lo ≤ lo + k - 1 ≤ hi;
    if lo = hi then return lo endif;
    mid = SPLIT (lo, hi);
    if k ≤ mid - lo then SELECT (k, lo, mid - 1)
     else if k = mid - lo + 1 then return mid
     else SELECT(k - mid + lo - 1, mid +1, hi)
    endif.
```

The expected running time for m input points is $O(m)$, with a reasonably small constant of multiplicity. The operation SELECT is called repeatedly, with an average size of N being equal to about m_0. Because the SELECT operation is typically executed a large number of times, it is important that it be optimized for this input point size.

Operations to construct stars, stage B, can be considered as a sequence of operations that include:

(B1) Using points in S_i to estimate the normal $\mathbf{n}_i$ and the estimated tangent plane $T_i : \langle \mathbf{x}, \mathbf{n}_i \rangle = 0$ at p_i;

(B2) Projecting the points in S_i to form the set S_i' of weighted points in T_i, which contains points p_i'; and

(B3) Computing the star of p_i' in the weighted Delaunay triangulation of S_i'.

It is preferred that operations B1, B2 and B3 are performed for each point $p_i \in S$. Each edge of the resulting triangulation can occur in up to two stars and each triangle can occur in up to three stars. Moreover, as explained more fully hereinbelow, weights are preferably used to counteract distortion caused by the projection of the points in S_i to form the set S_i' of weighted points in T_i.

The operations B1 assume that each set of near points S_i is sampled from a small and smooth neighborhood of the point p_i, and that the points $p_j \in S_i$ lie close to the plane tangent to the surface and passing through p_i. Because the surface to be reconstructed is not known, the locations of planes tangent to the surface are also not known. Nonetheless, the tangent planes may be estimated from respective sets of near points S_i. In particular, each estimated tangent plane T_i is computed as the two-dimensional linear subspace of $\mathbb{R}^3$ that minimizes the sum of square distances to the points p_j-p_i, over all $p_j \in S_i$. The definitions of T_i as the estimated tangent plane at p_i and n_i as the estimated normal at p_i are illustrated in FIG. 1.

The operations B2 include determining weighted points in T_i. In particular, for each point $p_j \in S_i$, the projected point $p_j' = (p_j'', w_j)$ is the weighted point in T_i, where:

$$p_j'' = (p_j - p_i) - \langle p_j - p_i, \mathbf{n}_i \rangle \mathbf{n}_i$$

is the orthogonal projection of p_j-p_i onto T_i and $w_j = -\langle p_j - p_i, \mathbf{n}_i \rangle^2$ is the negative square distance of that point from T_i. We use the weight to counteract the distortion of the inter-point distances. To explain this, we define the weighted square distance of a point $x \in T_i$ from p_j' as:

$$\pi_j(x) = ||x - p_j''||^2 - w_j,$$

which is the Euclidean square distance of x from p_j. As described in a textbook by H. Edelsbrunner, entitled "Geometry and Topology for Mesh Generation," Cambridge Univ. Press (2001), the disclosure of which is hereby incorporated herein by reference, a weighted Voronoi region of p_i' is the set of points $x \in T_i$ whose weighted square distance to p_i' is no larger than any other weighted point, $V_i = \{x \in T_i \mid \pi_i(x) \leq \pi_j(x), \forall j\}$. It is also the intersection of the three-dimensional (unweighted) Voronoi cell of p_i with the plane T_i. The rationale is that as long as T_i intersects the Voronoi cell for p_i in the same set of facets and edges as the hypothetical surface, the star of p_i' in the weighted Delaunay triangulation (the dual of the weighted Voronoi diagram) is the projection of the star of p_i in the restricted Delaunay triangulation (the dual of the intersection between the three-dimensional Voronoi diagram and the hypothetical surface). The concept of a restricted Delaunay triangulation is more fully described in the article by H. Edelsbrunner and N.R. Shah, entitled "Triangulating Topological Spaces," Internat. J. Comput. Geom Appl., Vol. 7, pp. 365-378 (1997), the disclosure of which is hereby incorporated herein by reference. In other words, the stars in the two-dimensional weighted Delaunay triangulations are the closest representations to an ideal reconstruction, which is the restricted Delaunay triangulation.

Understanding the operations B3 for computing the star of p_i' in the weighted Delaunay triangulation of S_i' requires a basic understanding of weighted Delaunay triangulations in a plane, which will now be provided. The weighted square distance to two weighted points $p_i' = (p_i'', w_i)$ and $x' = (x,w)$, can be generalized as:

$$\pi_i(x') = ||p_i'' - x||^2 - w_i - w.$$

The two weighted points are orthogonal if $\pi_i(x') = 0$, which in geometric terms means that the circles centered at p_i'' and x with radii $w_i^{1/2}$ and $w^{1/2}$ intersect at a right angle. The two weighted points are considered closer than orthogonal if $\pi_i(x') < 0$ and farther than orthogonal if $\pi_i(x') > 0$. In the plane, for any three weighted points p_i', p_j' and p_k', there is a unique weighted point x' that is orthogonal to all three. This weighted point x' is the orthocenter of p_i', p_j' and p_k'. If S_i' is the collection of weighted points in $\mathbb{R}^2$, by duality to the weighted Voronoi diagram, the weighted Delaunay triangulation of S_i' consists of all triangles $p_i''p_j''p_k''$ for which the orthocenter of p_i', p_j' and p_k' is farther than orthogonal to all other weighted points in S_i'. As described at section 1.4 of the aforementioned textbook by H. Edelsbrunner, the genericity of the set of weighted points can be simulated to avoid ambiguities in the characterization of the weighted Delaunay triangulation. An example of a two-dimensional weighted Delaunay triangulation **40** is illustrated by FIG. 4, where the shaded star of p_i' within the weighted Delaunay triangulation of S_i' is either an open disk or an open half-disk.

The star of a projected point p_i', denoted herein as St p_i', consists of the point p_i' and all edges and triangles in D_i' that contain p_i' as a vertex. The underlying space of the star is the union of the interiors of its simplices, as defined by the following relationship:

$$|\mathrm{St}\, p_i'| = \cup_{\sigma \in \mathrm{St}\, p_i'} \mathrm{int}\, \sigma.$$

Two cases can be distinguished, based on whether the projected point p_i' is an interior vertex or a boundary vertex. If p_i' is an interior vertex of the weighted Delaunay triangulation, then the edges and triangles in the star alternate and close a ring about the vertex. In this case, the underlying space is an open disk. However, if p_i' is a boundary vertex of the triangulation, then the edges and triangles still alternate, but form only a sequence about the vertex. In this case, the underlying space is an open half-disk. Both cases are illustrated by the shaded stars in FIG. 4. When the projection is not important or reversed, then reference may be made to the star of p_i instead of the star of p_i'.

The operations B3 include computing the star of p_i' in a counterclockwise order around p_i'. As described herein, the distance between two weighted points will be computed as the weighted square distance between the two weighted points. These operations begin by renaming the weighted points such that $q_0 = p_i'$, q_1 is the weighted point closest to q_0, and $q_1, q_2, \ldots, q_{k-1}$ is the counterclockwise order of the weighed point around q_0. An ambiguity in the order arises when two weighted points lie on the same half-line emanating from q_0 and this ambiguity is resolved by throwing away the weighted point farther from q_0. It is convenient to repeat $q_k = q_1$ at the end of the ordering. To distinguish the interior from the boundary vertex case, the orientation of point triplets is tested. Using Greek letters for the x and y Cartesian coordinates in T_h, the orientation of the point triplet qrs is the sign of the determinant of the matrix Γ, where $q = (\psi_1, \psi_2)$, $r = (\rho_1, \rho_2)$ and $s = (\sigma_1, \sigma_2)$:

$$\Gamma = \begin{bmatrix} 1 & \psi_1 & \psi_2 \\ 1 & \rho_1 & \rho_2 \\ 1 & \sigma_1 & \sigma_2 \end{bmatrix}.$$

A positive orientation means that a left-turn is taken at r, coming straight from q and going straight to s. The interior vertex case is characterized by the property that all triplets $q_0 q_j q_{j+1}$ have positive orientation. In the

boundary vertex case, there is precisely one index j for which $q_0q_jq_{j+1}$ does not have positive orientation. The vertices are then relabeled so that q_{j+1} is the first and q_j is the last in the counterclockwise ordering around q_0. In contrast to the interior vertex case, the first vertex is not repeated at the end of the ordering.

With these preparations, the operations for constructing the star are the same for both interior and boundary vertices and are performed incrementally. For each new weighted point, all triangles whose orthocenters are closer than orthogonal are removed and then one new triangle is added to the star. At any moment, the star is a sequence of triangles, as illustrated in FIG. 5. In FIG. 5, if all weights w_i are assumed to be zero, the new point q_5 is closer than orthogonal to the orthocenters of the last triangle $q_0q_3q_4$ in the shaded partial star **50**. That last triangle is removed before q_5 is added as a vertex of the new last triangle $q_0q_3q_5$. The operations PUSH, POP, TO and ISEMPTY are used to manipulate an initially empty stack that stores the sequence of vertices on the boundary of the partial star:

```
PUSH^2 (q_1, q_2);
for j = 3 to k do
  loop r, s = TOP^2;
    if TOOCLOSE(q_0, r, s, q_j) then POP
    else PUSH (q_j); exit
    endif
  forever
endfor.
```

The boolean function TOOCLOSE tests whether or not the point q_j is closer than orthogonal to the orthocenters of q_0, r, and s. Using again Greek letters for the coordinates and the weights, the matrix Λ is defined as:

$$\Lambda = \begin{bmatrix} 1 & \psi_1 & \psi_2 & \psi_1^2 + \psi_2^2 - \psi_w \\ 1 & \rho_1 & \rho_2 & \rho_1^2 + \rho_2^2 - \rho_w \\ 1 & \sigma_1 & \sigma_2 & \sigma_1^2 + \sigma_2^2 - \sigma_w \\ 1 & \tau_1 & \tau_2 & \tau_1^2 + \tau_2^2 - \tau_w \end{bmatrix},$$

for $q = q_0$, r, s and $t = q_f$. The weighted point t (= (τ_1, τ_2)) is orthogonal to the orthocenter of qrs if and only if det $\Lambda = 0$. The triplet qrs has positive orientation, by construction, and it follows that the determinant of the upper left three-by-three submatrix (in the above matrix Λ) is positive. Hence, t is farther than orthogonal to the orthocenter if and only if det $\Lambda > 0$. The following operations are thus defined:

boolean TOOCLOSE (q, r, s, t)
return det $\Lambda < 0$.

The running time of the star construction operations is O(k log k) for sorting plus O(k) for constructing the star as described above.

The operations to compute stars may result in stars that share triangles and edges with other stars and stars that conflict with other stars, because the operations are performed independently in the various estimated tangent planes. In the event a conflict is present, the edges and triangles that are in conflict are eliminated and the remainder of edges and triangles that are not in conflict are merged into a single surface description.

Operations to merge stars, stage C, can be treated as a sequence of four sub-operations that include:

(C1) Sorting F, which is a list of all triangles in the stars, and remove all triangles that are not in triplicate;

(C2) Connecting the remaining triangles to form a triangulated pseudomanifold;

(C3) Sorting E, which is a list of edges in stars that do not belong to any triangles in the pseudomanifold, and remove all edges that are not in duplicate; and

(C4) Adding the remaining edges to the triangulated pseudomanifold.

The representation of the pseudomanifold created in operations C2 and C4 may be referred to as a trist data structure. In the operation C1 to sort triangles, each triangle is represented by the ordered triplet of indices of its vertices, *ijk* with $i < j < k$. The sort operation is performed lexicographically:

$$ijk \text{ precedes } i'j'k' \text{ if } \begin{cases} i < i', \\ i = i' \text{ and } j < j', \text{ or} \\ i = i', j = j', \text{ and } k < k'. \end{cases}$$

The use of contiguous integers suggests the use of a radix sort operation, rather than a comparison-based sorting operation. To describe the radix sort operation, n is defined as the number of points in S and $B[1..n]$ is defined as a linear array of buckets. Each bucket is initially an empty stack of integer pairs. In the first phase, the triangles are spread using the smallest of the three vertex indices as the address in B. The operation $\text{PUSH}_i(j,k)$ is used to add the pair jk to the i-th bucket:

```
forall i do
    forall triangles p_i p_j p_k ∈ St p_i do
      rename indices such that i <j <k; PUSH_i (j,k)
    endfor
endfor.
```

A single vertex belongs to at most some constant number of triangles. The sorting operation can therefore be finished by calling quicksort for each bucket without paying a logarithmic term in comparison to additional phases

of a radix sort. After sorting, B[i] contains the triangles *ijk* lexicographically sorted by *jk*. The triangles that are not in triplicate can thus be eliminated by scanning. The operations POP_i, TOP_i, and $ISEMPTY_i$ can be used to manipulate the *i*-th bucket. The triangles that occur three times are collected in an initially empty list *F*, which is extended using function ADD. The following pseudocode illustrates these operations:

```
for i = 1 to n do
    while not ISEMPTY_i do jk = POP_i;
     if TOP_i = jk then jk = POP_i;
         if TOP_i = jk then jk = POP_i; ADD (ijk) end if
     endif
    endwhile
endfor.
```

The trist data structure is an array of (unordered) triangles connected to each other by adjacency. In the operation C2, each unordered triangle with vertices p_i, p_j, and p_k is represented by its six ordered versions. As illustrated by FIG. 6, each ordered version of an unordered triangle stores a pointer *fnext* to the next triangle in the ring around the directed edge **60a-60f** identified by the first two vertices in the ordering. By construction, each edge belongs to at most two triangles, which implies that three of the six *fnext* pointers are redundant. We find matching pairs of triangles by sorting the 3*f* (unordered) edges of the *f* triangles in *F* using the radix sort operation. Let E_2 be the list of edges obtained after removing the ones that occur only once. In this list, we represent each edge by the ordered pair of vertex indices, *ij* with $i < j$, and a *tri* pointer to the triangle responsible for its existence in E_2. The triangles are finally matched by scanning E_2. If $2e_2$ is defined as the length of E_2, then the following operations can be performed to match up all triangles:

```
for l = 1 to e_2 do
    CONNECT (E_2[2 l - 1].tri,E_2[2 l].tri)
```

endfor.

Besides the edges that are shared by two triangles, boundary edges are provided in the resulting pseudomanifold. For each boundary edge $p_i p_j$, a triangle $p_i p_j \omega$ is constructed, where ω is a new dummy vertex. The dummy triangles **70** connecting ω to boundary edges are illustrated in FIG. 7. In particular, FIG. 7 illustrates five dummy triangles **70a-70e**, four of which (i.e., **70a-70d**) connect ω to boundary edges and one of which (i.e., **70e**) connects ω to a principal edge in the star of p_i. The boundary edges are exactly the ones removed from E_2. Assuming the boundary edges are collected in another list, E_1, the dummy triangles are constructed in a single scan, as illustrated by the below operations:

for l = 1 to e_1 do
    let ij be the index pair in $E_1[l]$;
    create $p_i p_j \omega$; CONNECT ($E_1[l]$.tri, $p_i p_j \omega$)
endfor.

The operations C3 include adding principal edges. In these operations, all edges that belong to the stars of both their endpoints are accepted as members of the pseudomanifold. The edges that belong to one or two accepted triangles are already part of the pseudomanifold, but the principal edges that belong to no accepted triangles need to be added. Each principal edge $p_i p_k$ is represented by the dummy triangle $p_i p_k \omega$ shown as dummy triangle **70e** in FIG. 7. All principal edges are found by radix sorting the edges in the collection of stars constructed in accordance with operations B3. The edges that are not in duplicate are removed along with edges that are in E_1 or in E_2. The resulting list, E_0, stores all principal edges. Similar to the boundary edges, the principal edges are added to the pseudomanifold in a single scan, as illustrated by the following operations:

for l = 1 to e_0 do
    let ij be the index pair in $E_0[l]$; create $p_i p_j \omega$

endfor.

It is possible that a problematic case of two 'crossing' principal edges may occur. For example, if p_i, p_j, p_k and p_l form a square, then the distortions caused by the projections of these points into four estimated tangent planes may create a contradictory agreement between diagonally opposing vertices. This is shown by FIG. 8, where two 'crossing' principal edges **80a** are shown on the left. As also shown on the right side of FIG. 8, a similarly problematic case may also occur between two accepted triangles **80b**. The case of 'crossing' edges can be avoided relatively inexpensively by prohibiting the occurrence of a principal edge p_ip_k for which the two neighboring edges p_ip_j and p_ip_l in the star of p_i are connected by another principal edge, namely p_jp_l. Such cases are again found using a radix sort operation and the involved edges are removed from E_0 before they can be added to the pseudomanifold.

Operations C4 to establish order and to add the remaining edges to the triangulation of the pseudomanifold will now be described. As described above, each star St p_i is represented by a list storing the vertices on the boundary in order. These lists are used to connect the dummy triangles to each other. First, boundary and principal edges in the star are identified. Each boundary edge either starts or ends a hole when the star is read in a counterclockwise order. By definition, a principal edge both ends a hole and starts a new one. The buckets $B[1..n]$ are used again. The operations include storing in $B[i]$ all indices k of vertices that define dummy triangles $p_ip_k\omega$. The buckets are sorted using quicksort, as described above, and each index is stored with a pointer to the corresponding dummy triangle. A given vertex index j can be located in $B[i]$ using a binary search operation. If $j \in B[i]$, then p_ip_j is either a boundary edge that starts a hole, a boundary edge that ends a hole, or a principal edge. The identity of p_ip_j can be determined by checking the non-null *fnext* pointers of the dummy triangle $p_ip_j\omega$, if any. The boolean operations STARTS and ENDS can be used to

express the test. The function $FIRST_i$ is also used to return the first vertex in the i-th star, and the function $NEXT_i$ is used to return the next vertex that defines a boundary or principal edge. After passing the last such vertex, function $NEXT_i$ returns null. To reduce the disk and half-disk cases to one, the first vertex of a half-disk is repeated at the end of the list, making it appear as a disk. These operations are described by the following operations:

```
for i = 1 to n do p_j = FIRST_i;
    repeat p_k = NEXT_i;
      if STARTS(p_j) then assert ENDS(p_k);
          CONNECT (p_i p_j ω, p_i p_k ω);
      endif; p_j = p_k
    until p_k = null
endfor.
```

The most time-consuming part of these operations is the classification of edges, which is done using a binary search of the sorted lists $B[i]$. The lengths of these lists is bounded from above by the constant $k_0 - 1$, which implies that searching takes only constant time. The order among the dummy triangles is thus established in a time proportional to the number of edges.

Post-processing operations to identify and fill holes, identified above as stage D, include multiple sub-operations that will now be described. Holes in a pseudomanifold may be caused by missing data or by conflicts between vertex stars. The operations described hereinbelow can be used to fill small and simple holes automatically, but large or complicated holes are typically left to a user to manually fill. The operations to fill holes include:

(D1) Finding holes by identifying boundary cycles;

(D2) Accepting holes that can be filled automatically; and

(D3) Filling accepted holes with triangulated polygons.

Operations to determine boundary cycles can be performed efficiently because the vertex stars are ordered. However, testing whether or not a boundary cycle (e.g., hole) can be filled automatically is typically a more complex operation and may depend on the type of shape being reconstructed and the application to which the reconstructed surface is to be applied. A few conservative heuristics can be used to determine whether or not a boundary cycle may be filled automatically. The complexity of the hole filling operations is typically proportional to the size of the hole to be filled.

Operations D1 for identifying boundaries include using the classification of edges as principal, boundary, or interior edges, as described above. Each boundary edge p_ip_j starts a hole in the star of one endpoint and ends a hole in the star of the other endpoint. A directed graph H is constructed that represents each principal edge p_ip_j in K by its two directed versions, p_ip_j and p_jp_i, and each boundary edge that starts a hole in St p_i and ends one in St p_j as the directed edge p_ip_j. Stated alternatively, the directed graph H is a directed version of the link of ω in K. The set of directed edges in H can be partitioned into directed cycles and the boundary cycles are identified as respective directed cycles. Let ωp_ip_j be a triangle in the star of ω such that p_ip_j is a directed edge in H. The cycle that contains p_ip_j can be traced by following *fnext* pointers. Function APPEND adds a new edge at the end of a list representing the traced cycle, as illustrated by the following operations:

```
while p_ip_j is unmarked do
    APPEND (p_ip_j); mark p_ip_j; ωp_ip_j = ωp_jp_i.fnext
endwhile.
```

Observe the permutation ωp_jp_i of ωp_ip_j used to indicate a different ordered version of the triangle. As illustrated in FIG. 9, the cycles are traced such that the holes lie locally to the left of the directed edges. We trace cycles until all directed edges in H are marked.

The operations D2 include accepting holes that can be filled automatically, which typically includes only relatively small and simple holes. The size of the holes can be measured either geometrically, as the length or the diameter, or combinatorially, as the number of directed edges of the boundary cycle. The size of the holes can be distinguished by introducing a size threshold. However, the distinction between simple and complicated holes is more intricate. A hole may be treated as a "simple" hole if its boundary cycle can be embedded in a plane.

Because of the nature of the operations used in the construction of a cycle, its embedding surrounds an open disk on its left, as shown in FIG. 10. This open disk represents the hole to be filled. The indices of the vertices that are encountered when a boundary cycle is traversed can be recorded. A single vertex may occur an arbitrary number of times, but an alternation of the form *..i..j..i..j..* is not possible. Thus, a proper boundary cycle is a Davenport-Schinzel cycle of order at most two. This can be illustrated simply by taking a circle and marking four points with alternating labels, *i, j, i, j*. The point *i* is then connected to point *i* by a path outside the circle. Similarly, the point *j* is connected to *j* by a path outside the circle. As long as the paths are drawn in general position, they will cross an odd number of times. The circle is then deformed into a boundary cycle so that the ends of each path become the same and the paths become closed curves. However, two closed curves in general position necessarily cross an even number of times, which is a contradiction.

An operation is used that decides whether or not a cycle *Z* of indices contains a forbidden alternation between two indices, *i* and *j*. It is convenient to cut Z open to form a sequence. A forbidden alternation defines two intervals, one from *i* to *i* and the other from *j* to *j*, that overlap but neither is contained in the other. Two intervals with this property are independent. In the first pass, the operation computes all intervals between contiguous occurrences of the same index. Each interval is represented by having its endpoints point to each other. In the second pass, the cycle *Z* is

scanned to see whether there is an independent pair of intervals. If the sequence is stored in an array $Z[1..m]$, each location l stores the index of a vertex, the left endpoint l- of the interval that ends at l, and the right endpoint l+ of the interval that starts at l. Both are positions in Z and the value zero is used to represent the non-existence of such endpoints. The operations, which maintain an initially empty stack of currently enclosing intervals, are described by the following operations:

```
boolean isSIMPLE (Z)
    for l = 1 to m do
      if l- ≠ 0 then [a, b] = POP;
          if [a, b] ≠ [l-, l] then return FALSE endif
      endif;
      if l+≠0 then PUSH ([l, l+]) endif
    endfor; return TRUE.
```

Function isSIMPLE is correct because if all intervals are either disjoint or nested, then the last interval pushed on the stack is the first one to be popped. The running time is proportional to the length of the cycle.

Operations D3 for triangulating holes will now be described. As holes get larger and more complicated, filling operations that get progressively more sophisticated are required. However, if only simple holes are considered, the operations may be efficiently performed. These hole filling operations create no new vertices and fill a hole with edges and triangles connecting the boundary cycle, Z. By restricting the operations to simple holes, these filling edges and triangles form the triangulation of a disk whose dual graph is a tree. The triangles that correspond to leaves can be referred to as ears. If Z has $m > 3$ edges, then there are at least two ears. The triangulation can thus be built by adding an ear at a time. More precisely, the operations find two consecutive edges p_ip_j and p_jp_k in Z, add the triangle $p_ip_jp_k$ and the edge p_ip_k to K, and substitute p_ip_k for p_ip_j, p_jp_k in Z. To produce a reasonable triangulation, the ears are prioritized by the angle

at the middle vertex, p_j. Because the hole lies locally to the left of p_ip_j, p_jp_k, the angle on that side in the projection is measured onto the estimated tangent plane. To avoid duplications, edges p_ip_k that are already part of the triangulation surrounding the hole are rejected. The operations use a priority queue for the edge pairs, which can be manipulated using the functions MINEXTRACT and CHANGEKEY (where p_j- and p_j+ are used to represent the predecessor and successor of p_j in Z):

```
while m > 3 do p_j = MINEXTRACT;
    if not IN K (p_j-, p_j+) then
      add p_j-p_jp_j+ and p_j-p_j+ to K;
      CHANGEKEY^2 (p_j-, p_j+); m = m -1
    endif
endwhile;
p_j = MINEXTRACT; add p_j-p_jp_j+ to K.
```

The running time for filling a hole bounded by a cycle with m edges is $O(m \log m)$.

The above-described operations for creating and merging stars will now be more fully described with respect to FIGS. 11-14. In particular, FIG. 11 illustrates a small set of points, including p_1 and p_2, that define a portion of a three-dimensional (3D) surface. In FIG. 12A, a first set of near points S_1 associated with the first point p_1 and a second set of near points S_2 associated with the second point p_2 are projected to respective tangent planes, shown as T1 and T2. The first set of near points S_1 and the second set of near points S_2 typically contain some points that are common to both sets. In the tangent plane T1, the projection of the first point, p_1', represents the starting point q_0 for creating the star of p_1'. Similarly, in the tangent plane T2, the projection of the second point, p_2', represents the starting point q_0 for creating the star of p_2'. Referring now to FIG. 12B, the first triangle in the star of p_1' is created by connecting the starting point q_0 to the nearest point in the tangent plane T1, shown as point q_1, by an edge. Then,

continuing in a counter-clockwise direction relative to the edge q_0q_1, the starting point q_0 is connected to the next closest point, shown as q_2. The points q_1 and q_2 are also connected by an edge to thereby define the first triangle $q_0q_1q_2$. The next nearest point in the counter-clockwise direction, q_3, is then identified. Referring now to FIG. 12C, an evaluation is then made to determine whether the point q_3 is within a circumcircle of the first triangle $q_0q_1q_2$, which is defined as a circle that passes through the vertices of the first triangle. If the point q_3 is within a circumcircle of the first triangle $q_0q_1q_2$, then the point q_3 is added as a vertex of a triangle in the star of $p_1'=q_0$ and the point q_2 is discarded. As illustrated by FIG. 12D, the sequence of operations illustrated by FIGS. 12B-12C are repeated until the star of p_1', which frequently has about six (6) triangles, is fully defined as an open disk or open half-disk.

Referring again to FIG. 12B, the first triangle in the star of p_2' is created by connecting the starting point q_0 to the nearest point in the tangent plane T2, shown as point q_1, by an edge. Then, continuing in a counter-clockwise direction relative to the edge q_0q_1, the starting point q_0 is connected to the next closest point, shown as q_2. The points q_1 and q_2 are also connected by an edge to thereby define the first triangle $q_0q_1q_2$. The next nearest point in the counter-clockwise direction, q_3, is then identified. An evaluation is then made to determine whether the point q_3 in FIG. 12C is within a circumcircle of the first triangle $q_0q_1q_2$. If the point q_3 is outside a circumcircle of the first triangle $q_0q_1q_2$, then the point q_3 is added as a vertex of a new triangle in the star of p_2' and the point q_2 is retained as a vertex. As illustrated by FIG. 12D, the sequence of operations illustrated by FIGS. 12B-12C are repeated until the star of p_2' is fully defined.

As illustrated by FIG. 12D, two triangles A and B, which share a common edge, are illustrated with heavy shading. The triangle A in the first tangent plane T1 and the triangle A in the second tangent plane T2 have vertices that map to the same three points, including the first point p_1, in the point set illustrated by FIG. 11. Similarly, the triangle B in the first tangent

plane T1 and the triangle B in the second tangent plane T2 map to the same three points, including the first point p_1, in the point set illustrated by FIG. 11. Accordingly, as illustrated by FIG. 13, the above-described edge and triangle sorting operations may be performed to merge the pair of triangles A together and merge the pair of triangles B together into a surface triangulation, containing the star of p_1 and the star of p_2.

Preferred operations for creating stars from points projected to a plane will now be more fully described with respect to FIGS. 14A-14G. In particular, FIGS. 14A-14B illustrate operations that may be used to determine how the projected point q_5 is to be connected to other points in the star of q_0 as the star, which is shown as an open half-disk, is created. In FIGS. 14A-14B, the partial star of q_0 is expanded by evaluating whether the next point q_5 in the sequence of points $q_0,q_1,q_2,q_3,q_4,q_5,q_0$ is inside or outside a circumcircle of a triangle defined by the two immediately preceding vertices, q_4 and q_3, and vertex q_0. Because the next point q_5 in the sequence is outside the illustrated circumcircle, the triangle $q_0q_4q_5$, illustrated as triangle D, is added and the star of q_0 is defined by triangles A-D. However, in FIG. 14C, the next point q_5 in the sequence of points $q_0,q_1,q_2,q_3,q_4,q_5,q_0$ is inside the circumcircle of $q_0q_3q_4$. Accordingly, the point q_4 is dropped from the sequence and the new triangle $q_0q_3q_5$ is added as a replacement for the triangle $q_0q_3q_4$. Thus, as illustrated by FIG. 14D, the star of q_0 is defined by triangles A-B and E.

Referring now to FIG. 14E, the introduction of projection weights adds complexity to the operations for determining whether a next projected point in a sequence $q_0q_1q_2q_3....q_nq_0$ is to be added as a vertex of a new triangle. When projection weights are considered, the preferred operations include determining whether or not the next projected point in the sequence, illustrated as points "a", "b" or "c", is closer than orthogonal to an orthocenter of an orthocircle of triangle $q_0q_3q_4$, where each of the vertices q_0, q_3 and q_4 of the triangle $q_0q_3q_4$ has respective non-zero weights associated therewith that are function of projection distance (e.g., proportional to (projection

distance)^2). The magnitude of each respective weight is illustrated as proportional to a radius of a circle surrounding a respective point. As illustrated by FIG. 14E, each of the weighted points "a" and "b" appear to be closer than orthogonal (c.t.o) and point "c" appears to be farther than orthogonal (f.t.o). To determine conclusively whether or not a respective point is closer than orthogonal, the value of the det Λ can be determined for each weighted point to be evaluated, as described more fully hereinabove. For each case where det $\Lambda < 0$, the weighted point *t* is treated as being closer than orthogonal to the orthocenter of the triangle *qrs* and for each case where det $\Lambda > 0$, the weighted point *t* is treated as being farther than orthogonal. As described more fully in section 1.4 of the aforementioned textbook to H. Edelsbrunner, a geometric technique of symbolically perturbing a geometric input can be used advantageously to preclude inconsistencies in star building that may occur in cases where a weighted point is found to be orthogonal to the orthocenter (i.e., det $\Lambda = 0$).

The operations for determining det Λ can be understood geometrically by considering the two cases illustrated by FIGS. 14F-14G, for two points p and q. In both cases, the point q is orthogonal to the orthocenter p if:

$$||p-q||^2 - r^2 - s^2 = 0$$

FIG. 14F illustrates the real-real case where (r^2, $s^2 > 0$). In this case, the exterior angle α extending between the tangents to the circles surrounding points p and q (at the point of intersection between the two circles) can be evaluated to determine whether or not point q is closer than orthogonal to the orthocenter p, as shown by the following relationship:

$$\alpha \begin{cases} < 90^\circ \, f.t.o \\ = 90^\circ \, orthogonal \\ > 90^\circ \, c.t.o \end{cases}$$

FIG. 14G illustrates the real-imaginary case where ($r^2 > 0$, $s^2 < 0$). In this case, the interior angle α can be evaluated in accordance with the above relationships to determine whether or not point q is closer than orthogonal to the orthocenter p. The real-imaginary case presents the possibility of having a point q that is physically within an orthocircle centered about the orthocenter p, but is nonetheless farther than orthogonal to the orthocenter.

Referring now to FIG. 15, preferred high-level operations **100** for modeling a three-dimensional (3D) surface include determining a plurality of stars from a plurality of points in a 3D point set that at least partially describes the 3D surface, Block **110**, and then merging the plurality of stars into a digital model of the 3D surface, Block **120**. The operations **100** may be performed by a plurality of embodiments. In particular, FIG. 16 illustrates operations **200** for modeling a 3D surface that include identifying a subset of near points for each of a plurality of points in a 3D point set, Block **210**. This 3D point set may take the form of a point cloud data file, with each data point being identified by its Cartesian coordinates. The point cloud data file need not possess connectivity information that links or defines relationships between respective points therein. The point cloud data files may be provided in an ASCII xyz data format by conventional digitizers, including those manufactured by Cyberware™, Digibotics™, Laser Design™, Steinbichler™, Genex™ and Minolta™, for example. The data files may describe 3D surfaces that are closed. As will be understood by those skilled in the art of three-dimensional geometry, all closed 3D surfaces are either star-shaped or non star-shaped. Closed surfaces are "star" shaped if and only if there exists at least one point on the interior of the volume bounded by the closed surface from which all points on the surface are visible. All other surfaces are non star-shaped. Examples of star-shaped surfaces include a cube, a sphere and tetrahedron. Examples of non star-shaped surfaces include toroids (e.g, donut-shaped) and closed surfaces having tunnels and handles.

The operations **200** of FIG. 16 also include projecting a plurality of points from each subset of near points to a respective estimated tangent plane, Block **220**, and then determining a respective star from each set of projected points on an estimated tangent plane, Block **230**. As described above, the operations to determine a star from a set of projected points preferably includes assigning weights based on projection distance to at least a plurality of the projected points and using these weights to determine whether a projected point is to be a vertex of a triangle within the star or is to be discarded. The stars associated with each of a plurality of tangent planes are then merged into a 3D surface triangulation of the 3D point set, Block **240**. As illustrated by FIG. 17, these operations to merge stars, Block **240**, preferably include sorting triangles within the plurality of stars and removing those sorted triangles that are not in triplicate, Block **242**. The remaining triangles that are not removed are then connected to define a triangulated pseudomanifold, Block **244**. Operations may also be performed to sort those edges within the plurality of stars that do not belong to any of the triangles in the triangulated pseudomanifold, and remove those sorted edges that are not in duplicate, Block **246**. The remaining edges that have not been removed are then added to the triangulated pseudomanifold, Block **248**.

Preferred operations **300** to model 3D surfaces may also include preprocessing operations that improve the quality of the 3D point set by, among other things, reducing noise and removing outliers, as illustrated by FIG. 18. The preprocessing operations may include determining a respective set of near points for each of a plurality of points in a 3D point set, Block **310**, and then fitting each set of near points with a respective approximating surface, Block **320**. A denoising operation may then be performed by moving each of the plurality of points in the 3D point set to the approximating surface that is associated with its respective set of near points, Block **330**.

More detailed embodiments of these preprocessing operations are illustrated by FIG. 19. In particular, operations **400** to model 3D surfaces may include determining an estimated normal for each of a plurality of points in a 3D point set that at least partially describes the 3D surface, Block **410**, and then estimating principal curvature directions on the 3D surface by evaluating a differential structure of the estimated normals associated with the plurality of points, Block **420**. A local neighborhood of each of the plurality of points is also classified in terms of its shape characteristic, Block **430**. Based on its classification, an approximating surface is determined for each of the local neighborhoods, Block **440**. The quality of the 3D point set is then improved by moving each of the plurality of points to a respective approximating surface that is associated with a local neighborhood of the respective point, Block **450**.

Accordingly, the operations to model 3D surfaces may include operations to reduce noise within a 3D point set and then use the improved 3D point set to create and merge stars into a triangulated model of the 3D surface. Thus, as illustrated by FIG. 20, these modeling operations **500** may include determining a respective set of near points for each of a first plurality of points in a first 3D point set, Block **510**, and then fitting each set of near points with a respective approximating surface, Block **520**. An operation is then performed to generate a second 3D point set by denoising the first 3D point set, Block **530**. Operations are then performed to determine a plurality stars from a second plurality of points in the second 3D point set, Block **540**. The stars are then merged into a digital model of the 3D surface using preferred sorting and removal operations, Block **550**.

Referring now to FIG. 21, a general hardware description of a custom CAD/CAM workstation **600** is illustrated as comprising, among other things, software and hardware components that perform the operations described above, including those illustrated by FIGS. 15-20. The workstation **600** preferably includes a computer-aided design tool **620** that may accept a point cloud data set via a file **604**, a scanner **606**, data bus **602** or other

conventional means. A display **610** and a three-dimensional printer **608** are also preferably provided to assist in performing the operations of the present invention. The hardware design of the above described components **604**, **606**, **608** and **610** is well known to those having skill in the art and need not be described further herein. The workstation **600** preferably comprises a computer-readable storage medium having computer-readable program code embodied in the medium. This computer-readable program code is readable by one or more processors within the workstation **600** and tangibly embodies a program of instructions executable by the processor to perform the operations described herein.

In the drawings and specification, there have been disclosed typical preferred embodiments of the invention and, although specific terms are employed, they are used in a generic and descriptive sense only and not for purposes of limitation, the scope of the invention being set forth in the following claims. These claims include method, apparatus and computer program product claims. The method claims include recitations that may also be provided as recitations within apparatus and computer program product claims. In particular, the method claims may recite steps that can be treated as operations performed by apparatus and/or instructions and program code associated with computer program products.

THAT WHICH IS CLAIMED IS:

1. A method of modeling a three-dimensional (3D) surface, comprising the steps of:

determining a plurality of stars from a plurality of points p_i in a 3D point set S that at least partially describes the 3D surface, by projecting the plurality of points p_i onto planes T_i that are each estimated to be tangent about a respective one of the plurality of points p_i; and

merging the plurality of stars into a digital model of the 3D surface.

2. The method of Claim 1, wherein said determining step comprises identifying a respective subset of near points S_i for each of the plurality of points p_i.

3. The method of Claim 2, wherein said determining step comprises projecting a plurality of points p_j in each subset of near points S_i to a respective estimated tangent plane T_i.

4. The method of Claim 3, wherein said determining step comprises determining for each of a plurality of estimated tangent planes, T_i, a star of the projection of a respective point p_i onto the estimated tangent plane T_i.

5. The method of Claim 4, wherein the star of the projection of a respective point p_i onto the estimated tangent plane T_i constitutes a two-dimensional (2D) Delaunay triangulation.

6. The method of Claim 4, wherein the star of the projection of a respective point p_i onto the estimated tangent plane T_i constitutes a two-dimensional (2D) weighted Delaunay triangulation.

7. The method of Claim 6, wherein a distance between at least one point p_i and its orthogonal projection onto a respective estimated tangent plane T_i is non-zero.

8. The method of Claim 1, wherein said determining step comprises identifying a respective subset of near points S_i for each of the plurality of points p_i by storing the 3D point set S in an oct-tree.

9. The method of Claim 2, where:

$$S_i = \square_i(r_0) \cap N_i(k_0),$$

and $\square_i(r_0)$ is defined as the set of points $p_j \in S$ with an l_∞-distance at most r_0 from p_i and $N_i(k_0)$ is the set of k_0 points that are closest in Euclidean distance to p_i, including p_i itself, and k_0 is a positive integer.

10. The method of Claim 1, wherein said determining step comprises identifying a respective subset of near points S_i for each of the plurality of points p_i by determining a width of a near point search cube using a random sample $R \subset S$ and identifying those points in S that are within a respective near point search cube that is centered about each of the plurality of points p_i.

11. The method of Claim 1, wherein said determining step comprises identifying a respective subset of near points S_i for each of the plurality of points p_i by:

storing the 3D point set S in an oct-tree;

determining a width $2r_0$ of a near point search cube using a random sample $R \subset S$, where r_0 is a positive real number; and then, for each of the plurality of points p_i,

determining a subset of k_0 points that are closest in Euclidean distance to p_i and selecting from the subset all points that are also within a respective near point search cube that is centered about a corresponding point p_i and has a width equal to $2r_0$, where k_0 is a positive integer.

12. The method of Claim 1, wherein said determining step comprises identifying a respective subset of near points S_i for each of the plurality of points p_i by:

storing the 3D point set S in an oct-tree;

determining a width $2r_0$ of a near point search cube using a random sample $R \subset S$, where r_0 is a positive real number that equals a minimum value of r for which an average of a yield is greater than or equal to m_0, where m_0 is a positive constant and the yield equals the number of points in S that are within a near point search cube of width 2r centered about a respective point in the random sample R; and then, for each of the plurality of points p_i in the 3D point set S,

determining a subset of k_0 points that are closest in Euclidean distance to p_i and selecting from the subset all points that are also within a respective near point search cube that is centered about a corresponding point p_i and has a width equal to $2r_0$, where k_0 is a positive integer.

13. The method of Claim 11, where m_0 is about equal to 100 and k_0 is about equal to 30.

14. A method of modeling a three-dimensional (3D) surface, comprising the steps of:

determining a plurality of stars from a plurality of points p_i in a 3D point set S that at least partially describes the 3D surface, by projecting each of the plurality of points p_i onto a respective plane; and

merging the plurality of stars into a model of the 3D surface by eliminating edges and triangles from the plurality of stars that are in conflict and merging nonconflicting edges and triangles from the plurality of stars into a 3D surface triangulation.

15. The method of Claim 14, wherein said merging step comprises:

sorting triangles within the plurality of stars and removing those sorted triangles that are not in triplicate;

connecting the sorted triangles that have not been removed to define a triangulated pseudomanifold as a two-dimensional simplicial complex in which edges and triangles of a star that share a vertex form a portion of an open disk;

sorting edges within the plurality of stars that do not belong to any of the triangles in the triangulated pseudomanifold and removing those sorted edges that are not in duplicate; and

adding the sorted edges that have not been removed to the triangulated pseudomanifold.

16. The method of Claim 14, wherein said merging step comprises:

sorting triangles within the plurality of stars and removing those sorted triangles that are not in triplicate.

17. The method of Claim 16, wherein said merging step further comprises:

connecting the sorted triangles that have not been removed to define a triangulated pseudomanifold as a two-dimensional simplicial complex.

18. The method of Claim 17, wherein said merging step further comprises:

sorting edges within the plurality of stars that do not belong to any of the triangles in the triangulated pseudomanifold and removing those sorted edges that are not in duplicate; and

adding the sorted edges that have not been removed to the triangulated pseudomanifold.

19. A method of modeling a three-dimensional (3D) surface, comprising the steps of:

determining a plurality of triangulated neighborhoods from a plurality of points in a 3D point set that at least partially describes the 3D surface, by projecting each of the plurality of points and one or more neighboring points in the 3D point set to a respective plane; and

merging the plurality of triangulated neighborhoods into a digital model of the 3D surface.

20. The method of Claim 19, wherein said determining step comprises projecting each of the plurality of points and one or more neighboring points in the 3D point set to a respective tangent plane.

21. A method of modeling a surface of an object, comprising the steps of:

projecting each point and corresponding set of one or more neighboring points in a point set to a respective plane;

determining a star for each plane; and

merging the stars into a surface triangulation.

22. The method of Claim 21, wherein said projecting step comprises projecting each point and corresponding set of one or more neighboring points in a point set to a respective plane that is estimated to be tangent about the point.

23. The method of Claim 21, wherein said step of determining a star for each plane comprises determining a star having vertices that are weighted as a function of projection distance for each plane.

24. A method of modeling a three-dimensional (3D) surface, comprising the steps of:

determining an estimated normal for each of a plurality of points in a 3D point set that at least partially describes the 3D surface;

evaluating a differential structure of the estimated normals associated with the plurality of points to estimate principal curvature directions on the 3D surface and classify a respective local neighborhood of each of the plurality of points in terms of its shape characteristic;

determining a respective approximating surface for each of the local neighborhoods; and

denoising the 3D point set by moving each of the plurality of points to a respective approximating surface that is associated with a local neighborhood of the respective point.

25. A method of modeling a three-dimensional (3D) surface, comprising the steps of:

determining a respective set of near points S_i for each of a plurality of points p_i in a 3D point set S that at least partially describes the 3D surface, where $S_i \subseteq S$;

determining a normal bundle for the 3D point set S by determining a respective plane h_i of best fit for each of the sets of near points S_i and a respective normal n_i for each of the planes h_i of best fit; and

determining a respective approximating surface for each of the sets of near points S_i using the normal bundle to estimate respective principal curvature directions for each of the sets of near points S_i.

26. A method of modeling a three-dimensional (3D) surface, comprising the steps of:

determining a respective set of near points S_i for each of a first plurality of points $p1_i$ in a first 3D point set S1 that at least partially describes the 3D surface, where $S_i \subseteq S1$;

fitting each set of near points S_i with a respective approximating surface;

denoising the first 3D point set S1 into a second 3D point set S2 by moving at least some of the first plurality of points $p1_i$ in the first 3D point set S1 to the approximating surfaces associated with their respective sets of near points S_i;

determining a plurality of stars from a second plurality of points $p2_i$ in the second 3D point set S2, by projecting the second plurality of points $p2_i$ onto planes T_i that are estimated to be tangent about a respective one of the second plurality of points $p2_i$; and

merging the plurality of stars into a digital model of the 3D surface.

27. The method of Claim 26, wherein said step of fitting each set of near points S_i with a respective approximating surface comprises fitting a first set of near points S_1 with a first approximating surface by:

determining respective planes h_j of best fit for each of a plurality of points p_j in the first set of near points S_1; and

determining an estimated normal n_j for each of the points p_j as a normal of its respective plane h_j of best fit.

28. The method of Claim 26, wherein said step of fitting each set of near points S_i with a respective approximating surface comprises fitting a first set of near points S_1 with a first approximating surface by:

determining respective planes h_j of best fit for each of a plurality of points p_j in the first set of near points S_1;

determining an estimated normal n_j for each of the points p_j as a normal of its respective plane h_j of best fit; and

classifying the first set of near points S_1 in terms of its shape characteristic, by determining estimates of principal curvature directions for a point $p1_i$ from a plurality of the estimated normals n_j.

29. The method of Claim 26, wherein said step of fitting each set of near points S_i with a respective approximating surface comprises classifying a shape characteristic of each set of near points S_i as plane-like and/or edge-like and/or corner-like.

30. A method of modeling a three-dimensional (3D) surface, comprising the steps of:

determining a respective set of near points for each of a plurality of points in a 3D point set that at least partially describes the 3D surface;

fitting each set of near points with a respective approximating surface that is a selected from a group consisting of cylinders and quadratic and/or cubic surfaces; and

denoising the 3D point set by moving each of the plurality of points in the 3D point set to the approximating surface associated with its respective set of near points.

31. A method of modeling a three-dimensional (3D) surface, comprising the steps of:

determining a respective set of near points for each of a first plurality of points in a 3D point set that at least partially describes the 3D surface; and

determining an estimated normal for each of the first plurality of points by:

determining a respective plane of best fit for each of the sets of near points; and

determining a normal for each of the planes of best fit.

32. A method of modeling a three-dimensional (3D) surface, comprising the steps of:

determining a respective set of near points for each of a first plurality of points in a 3D point set that at least partially describes the 3D surface;

determining a normal bundle by determining a respective plane of best fit for each of the sets of near points and a normal for each of the planes of best fit; and

determining from the normal bundle at least one respective principal curvature direction for each of the sets of near points.

33. A method of modeling a three-dimensional (3D) surface, comprising the step of:

denoising a 3D point set that at least partially describes the 3D surface by:

classifying a first neighborhood of points in the 3D point set S1 using a mass distribution matrix of the first neighborhood of points to estimate first normals associated with the first neighborhood of points and a normal distribution matrix of the first normals to estimate principal curvature directions;

fitting an approximate surface, which is selected from a group consisting of cylindrical, quadratic and cubic surfaces, to the first neighborhood of points; and

moving at least one point in the first neighborhood of points to the approximate surface.

34. A method of modeling a three-dimensional (3D) surface, comprising the steps of:

identifying a respective subset of near points for each of a plurality of points in a 3D point set that at least partially describes the 3D surface by:

determining dimensions of a near point search space using a random sample of the 3D point set; and

selecting, for each of the plurality of points, a respective set of points in the 3D point set that are within a respective near point search space that is oriented about a respective one of the plurality of points;

determining a plurality of stars from the plurality of points in the 3D point set by projecting the points in each subset of near points to a respective plane; and

merging the plurality of stars into a digital model of the 3D surface.

35. The method of Claim 34, wherein each near point search space comprises a space selected from the group consisting of cubes, elipsoids, spheres and parallelpipeds.

36. The method of Claim 34, wherein said step of determining a plurality of stars comprises determining a plurality of stars from the plurality of points in the 3D point set by projecting the points in each subset of near points to a respective estimated tangent plane.

37. A method of reconstructing a surface of an object from a three-dimensional (3D) point cloud data set S derived from scanning the object, comprising the steps of:

determining a respective subset of near points $S_i \subset S$ for each of a plurality of points $p_i \in S$;

estimating a tangent plane T_i for each subset of near points S_i;

projecting each subset of near points S_i onto its respective tangent plane T_i;

constructing a respective star of each of the plurality of points p_i from the projected points on each of the tangent planes T_i;

merging the stars associated with the tangent planes T_i into a 3D model of the surface by eliminating edges and triangles from the stars that are in conflict and merging nonconflicting edges and triangles from the stars into a 3D surface triangulation; and

filling one or more holes in the 3D surface triangulation.

38. A method of reconstructing a surface of an object from a three-dimensional (3D) point cloud, comprising the steps of:

determining for each of a first plurality of points in the point cloud a respective approximating surface that fits the point's neighborhood;

moving each of the first plurality of points to its respective approximating surface;

determining an estimated tangent plane for each of a second plurality of points that have been moved to a respective approximating surface;

projecting each of the second plurality of points and points in their respective neighborhoods to a respective one of the estimated tangent planes;

constructing stars from points projected to the estimated tangent planes; and

merging the stars into a surface triangulation.

39. The method of Claim 38, further comprising the step of filling one or more holes in the surface triangulation.

40. A method of reconstructing a surface of an object from a three-dimensional (3D) point cloud, comprising the steps of:

denoising the point cloud;

determining an estimated tangent plane for each of a plurality of points in the denoised point cloud;

projecting each of the plurality of points and other points in its respective neighborhood to a respective one of the estimated tangent planes;

constructing stars from points projected to the estimated tangent planes; and

merging the stars into a surface triangulation.

41. The method of Claim 40, further comprising the step of filling one or more holes in the surface triangulation by:

constructing a directed graph that represents each principal edge of the surface triangulation by its two directed versions and each boundary edge as a single directed edge; and

identifying a boundary cycle of at least one hole by partitioning the directed graph into directed cycles.

42. The method of Claim 41, wherein said step of identifying a boundary cycle is followed by the step of identifying simple holes.

43. The method of Claim 42, wherein said step of identifying simple holes comprises identifying holes having index cycles that are Davenport-Schinzel cycles of order less than three.

44. A method of denoising a three-dimensional (3D) point set, comprising the steps of:

estimating directions of a local collection of normals associated with a local collection of data points in the 3D point set by determining eigenvectors of a mass distribution matrix of the local collection of data points; and

estimating directions of curvature associated with the local collection of data points by determining eigenvectors of a normal distribution matrix of the local collection of normals.

45. A method of modeling a three-dimensional (3D) surface, comprising the steps of:

moving each of a plurality of first points in a point set that at least partially describes the 3D surface to a respective approximating surface that is derived by evaluating a respective first point and a plurality of its neighboring points in the point set;

projecting at least one of the first points, which has been moved to an approximating surface, to a first plane that is estimated to be tangent about the at least one of the first points;

projecting a plurality of points in a neighborhood of the at least one of the first points to the first plane; and

generating a star from a plurality of projected points on the first plane.

46. A method of modeling a three-dimensional (3D) surface, comprising the step of:

determining a star of a first point in a 3D point set that at least partially describes the 3D surface, by:

projecting the first point and second, third and fourth points in a neighborhood of the first point to a plane;

assigning respective weights to each of the second, third and fourth points that are based on projection distance; and

evaluating whether the projection of the fourth point is within an orthocircle defined by a triangle having projections of the first, second and third points as vertices.

47. A method of modeling a three-dimensional (3D) surface, comprising the step of:

determining a first star of a first point in a 3D point set that at least partially describes the 3D surface, by:

projecting the first point and first near points in a neighborhood of the first point to a first plane that is estimated to be tangent to the first point:

assigning respective weights to each of the projected first near points that are based on distances between the first near points and the projected first near points; and

connecting the projected first point and at least some of the projected first near points with triangles that share the projected first point as a vertex, by evaluating whether a next projected near point in a first sequence of projected first near points is closer than orthogonal to an orthocenter of a triangle having the projected first point and two of the projected first near points as vertices.

48. The method of Claim 47, further comprising the step of:

determining a second star of a second point in the 3D point set by:

projecting the second point and second near points in a neighborhood of the second point to a second plane that is estimated to be tangent to the second point:

assigning respective weights to each of the projected second near points that are based on distances between the second near points and the projected second near points; and

connecting the projected second point and at least some of the projected second near points with triangles that share the projected second point as a vertex, by evaluating whether a next projected near point in a second sequence of projected second near points is closer than orthogonal to an orthocenter of a triangle having the projected second point and two of the projected second near points as vertices.

49. A method of modeling a three-dimensional (3D) surface, comprising the step of:

sequentially connecting a neighborhood of projected points on a plane to a first projected point on the plane by evaluating whether at least one projected point in the neighborhood of projected points is closer than orthogonal to an orthocircle defined by a triangle containing the first projected point and two projected points in the neighborhood of projected points as vertices, with the neighborhood of projected points having weights associated therewith that are each a function of a projection distance between a respective projected point in the neighborhood of projected points and a corresponding point in a 3D point set that at least partially describes the 3D surface.

50. The method of Claim 49, wherein the connected neighborhood of projected points constitutes a weighted Delaunay triangulation.

51. The method of Claim 49, wherein the plane is estimated to be tangent to the 3D surface.

52. A method of modeling a three-dimensional (3D) surface, comprising the steps of:

projecting a first point in a 3D point set that at least partially describes the surface and a set of points in a neighborhood of the first point to a plane that is estimated to be tangent to the surface at the first point; and

creating a weighted Delaunay triangulation comprising triangles that share a projection of the first point in the plane as a vertex and include at least some of the projections of the set of points in the neighborhood of the first point as vertices that are weighted as a function of projection distance.

53. The method of Claim 52, wherein the vertices are weighted as a function of projection distance squared.

54. An apparatus for modeling a three-dimensional (3D) surface, comprising:

means for determining a plurality of stars from a plurality of points p_i in a 3D point set S that at least partially describes the 3D surface, by projecting the plurality of points p_i onto planes T_i that are each estimated to be tangent about a respective one of the plurality of points p_i; and

means for merging the plurality of stars into a digital model of the 3D surface.

55. The apparatus of Claim 54, wherein said determining means comprises means for identifying a respective subset of near points S_i for each of the plurality of points p_i.

56. The apparatus of Claim 55, wherein said determining means comprises means for projecting a plurality of points p_j in each subset of near points S_i to a respective estimated tangent plane T_i.

57. The apparatus of Claim 56, wherein said determining means comprises means for determining for each of a plurality of estimated tangent planes, T_i, a star of the projection of a respective point p_i onto the estimated tangent plane T_i.

58. The apparatus of Claim 57, wherein the star of the projection of a respective point p_i onto the estimated tangent plane T_i constitutes a two-dimensional (2D) weighted Delaunay triangulation.

59. An apparatus for modeling a three-dimensional (3D) surface, comprising:

means for determining a plurality of stars from a plurality of points p_i in a 3D point set S that at least partially describes the 3D surface, by projecting each of the plurality of points p_i onto a respective plane; and

means for merging the plurality of stars into a model of the 3D surface by eliminating edges and triangles from the plurality of stars that are in conflict and merging nonconflicting edges and triangles from the plurality of stars into a 3D surface triangulation.

60. The apparatus of Claim 59, wherein said merging means comprises means for sorting triangles within the plurality of stars and removing those sorted triangles that are not in triplicate.

61. The apparatus of Claim 60, wherein said merging means further comprises:

means for connecting the sorted triangles that have not been removed to define a triangulated pseudomanifold as a two-dimensional simplicial complex.

62. The apparatus of Claim 61, wherein said merging means further comprises:

means for sorting edges within the plurality of stars that do not belong to any of the triangles in the triangulated pseudomanifold and removing those sorted edges that are not in duplicate; and

means for adding the sorted edges that have not been removed to the triangulated pseudomanifold.

63. A computer program product that models three-dimensional (3D) surfaces and comprises a computer-readable storage medium having computer-readable program code embodied in said medium, said computer-readable program code comprising:

computer-readable program code that determines a plurality of stars from a plurality of points p_i in a 3D point set S that at least partially describes the 3D surface, by projecting each of the plurality of points p_i onto a respective plane; and

computer-readable program code that merges the plurality of stars into a model of the 3D surface by eliminating edges and triangles from the plurality of stars that are in conflict and merging nonconflicting edges and triangles from the plurality of stars into a 3D surface triangulation.

64. The computer program product of Claim 63, wherein said computer-readable program code that merges the plurality of stars comprises:

computer-readable program code that sorts triangles within the plurality of stars and removes those sorted triangles that are not in triplicate;

computer-readable program code that connects the sorted triangles that have not been removed to define a triangulated pseudomanifold as a two-dimensional simplicial complex in which edges and triangles of a star that share a vertex form a portion of an open disk;

computer-readable program code that sorts edges within the plurality of stars that do not belong to any of the triangles in the triangulated pseudomanifold and removes those sorted edges that are not in duplicate; and

computer-readable program code that adds the sorted edges that have not been removed to the triangulated pseudomanifold.

65. A computer program product that models three-dimensional (3D) surfaces and comprises a computer-readable storage medium having computer-readable program code embodied in said medium, said computer-readable program code comprising:

computer-readable program code that projects a first point in a 3D point set that at least partially describes a 3D surface and a set of points in a neighborhood of the first point to a plane that is estimated to be tangent to the 3D surface at the first point; and

computer-readable program code that creates a weighted Delaunay triangulation comprising triangles that share a projection of the first point in the plane as a vertex and include at least some of the projections of the set of points in the neighborhood of the first point as vertices that are weighted as a function of projection distance.

66. A method of modeling a three-dimensional (3D) surface, comprising the steps of:

projecting a first point in a 3D point set that at least partially describes the surface and a set of points in a neighborhood of the first point to a plane that is estimated to be tangent to the surface at the first point; and

creating a weighted Delaunay triangulation comprising triangles that share a projection of the first point in the plane as a vertex and include at least some of the projections of the set of points in the neighborhood of the first point as vertices that are weighted as a function of projection distance, by evaluating whether or not one or more of the projections of the set of points in the neighborhood of the first point are closer than orthogonal to an orthocenter of a first triangle in the weighted Delaunay triangulation.

67. The method of Claim 66, wherein each of at least a plurality the vertices is weighted as a function of projection distance squared.

68. The method of Claim 66, wherein said creating step comprises evaluating a matrix containing coordinates of the vertices of the first triangle as entries therein.

69. The method of Claim 68, wherein said creating step comprises computing a determinant of the matrix.

70. The method of Claim 69, wherein the matrix is a 4x4 matrix; and wherein at least some of the entries in the matrix are functionally dependent on the weights associated with the vertices of the first triangle.

71. A surface modeling apparatus, comprising:

means for performing the method of any one of claims 1-53 and 66-70.

72. A computer program product readable by a machine and tangibly embodying a program of instructions executable by the machine to perform the method of any one of claims 1-53 and 66-70.

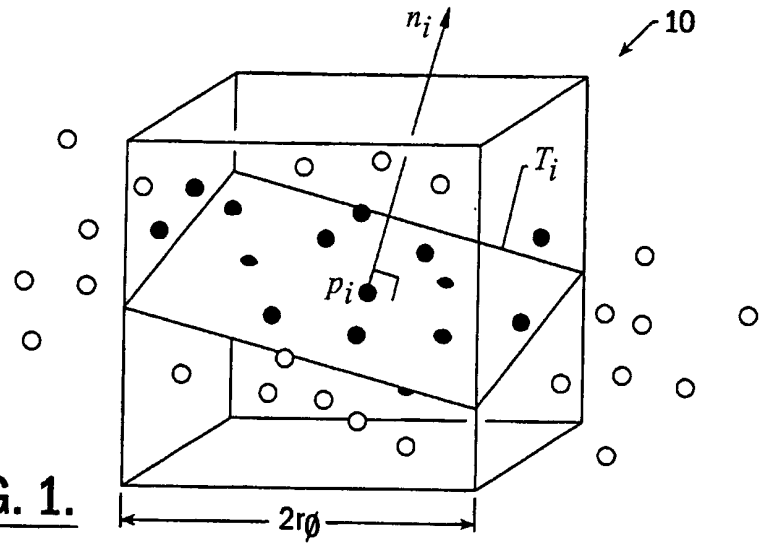

FIG. 1.

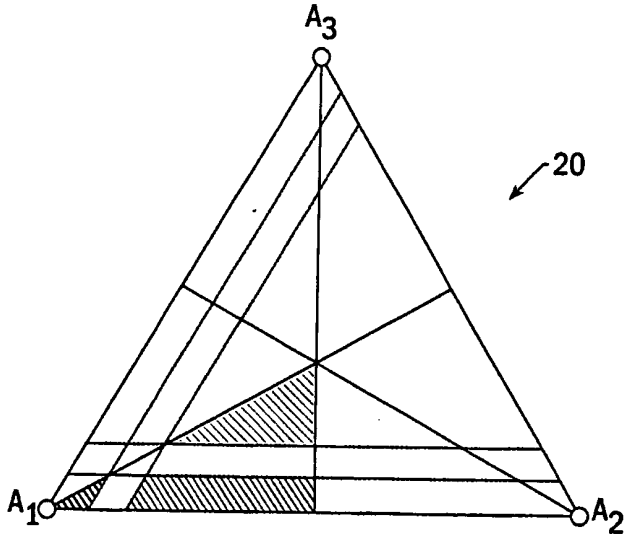

FIG. 2.

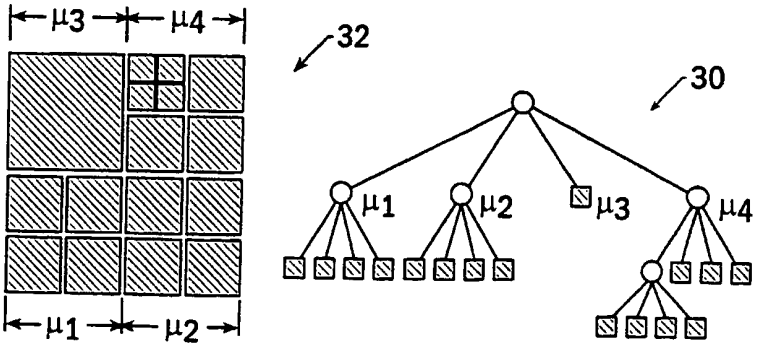

FIG. 3.

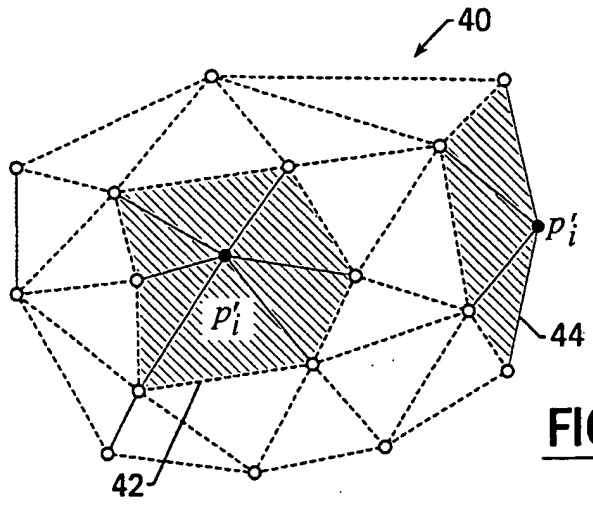

FIG. 4.

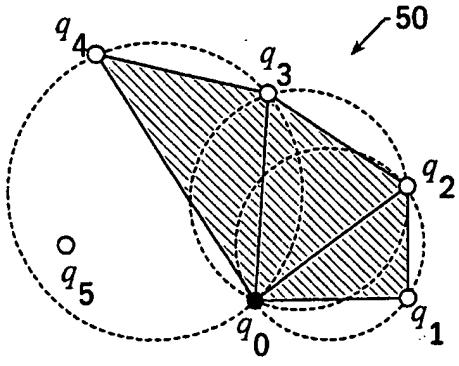

FIG. 5.

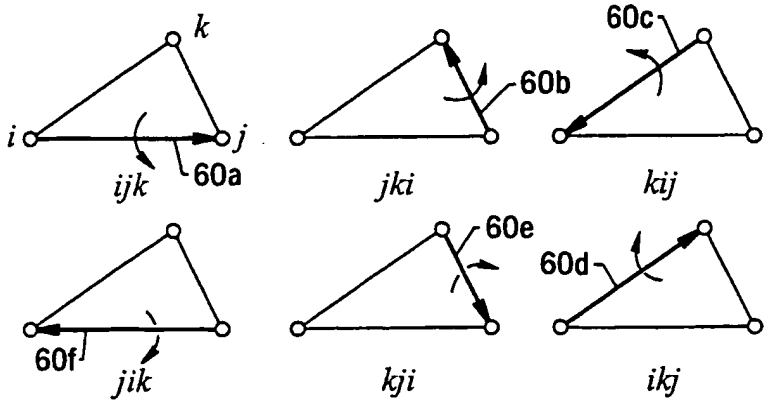

FIG. 6.

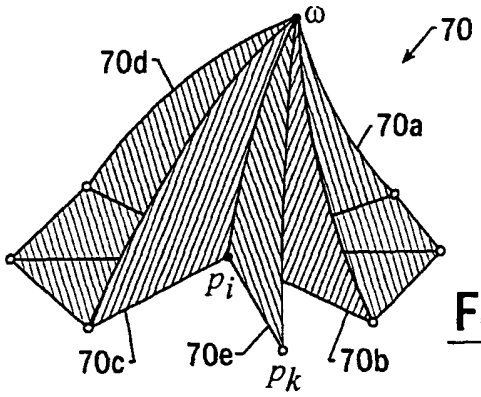

FIG. 7.

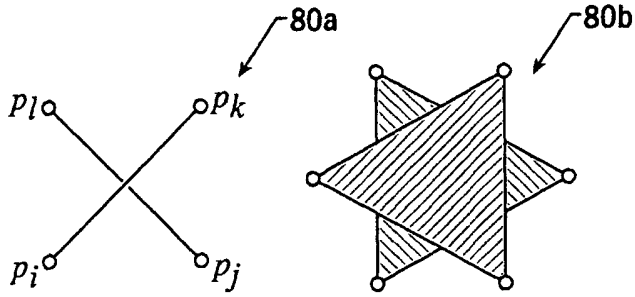

FIG. 8.

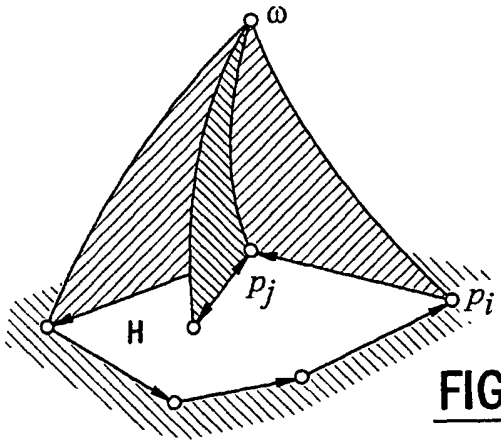

FIG. 9.

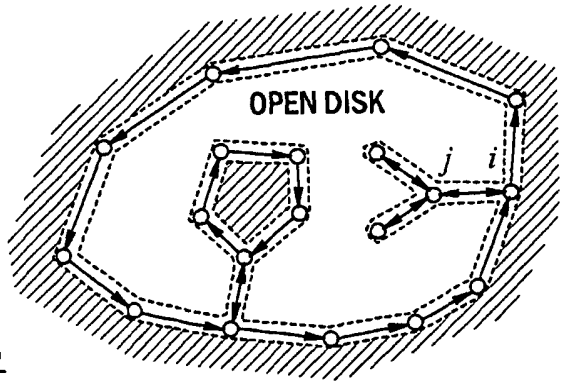

FIG. 10.

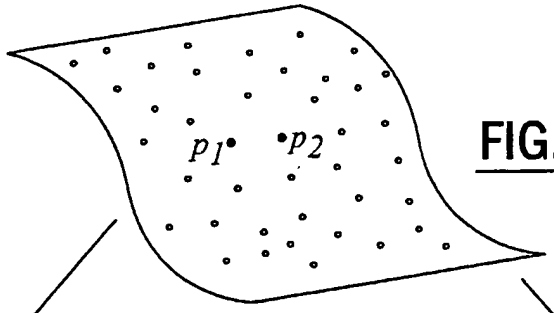

FIG. 11.

Project the sets of near points, S_1 and S_2, onto the tangent planes, T_1 and T_2.

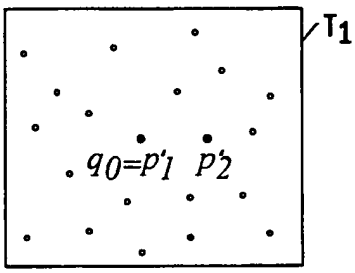

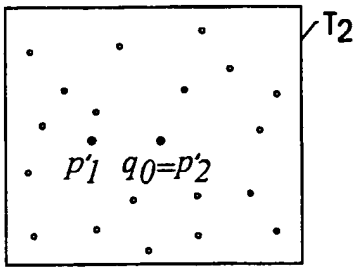

FIG. 12A.

CREATE 1st TRIANGLE $q_0q_1q_2$

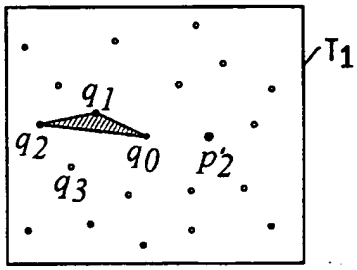

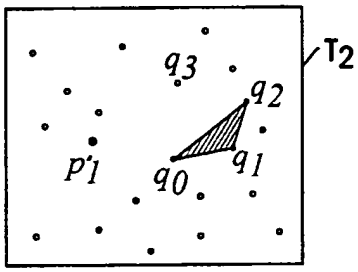

FIG. 12B.

REMOVE q_2 AND ADD $q_0q_1q_3$

ADD $q_0q_2q_3$

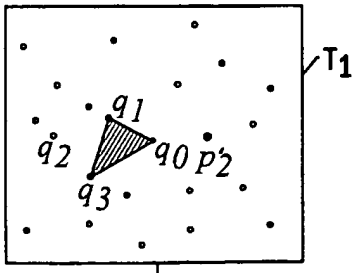

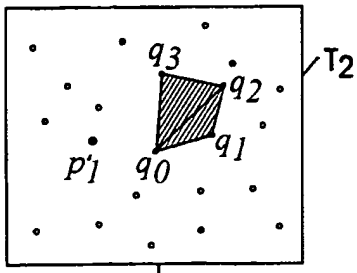

FIG. 12C.

ITERATE TO COMPLETE STAR OF p'_1

ITERATE TO COMPLETE STAR OF p'_2

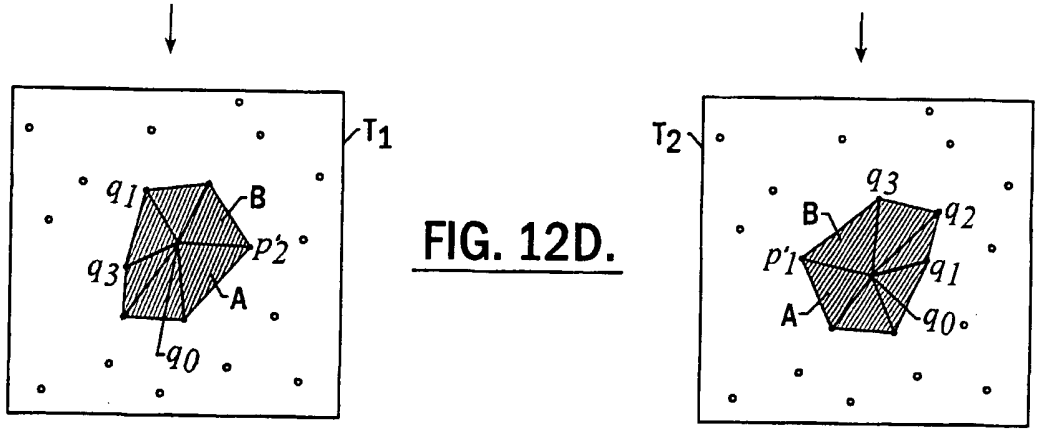

FIG. 12D.

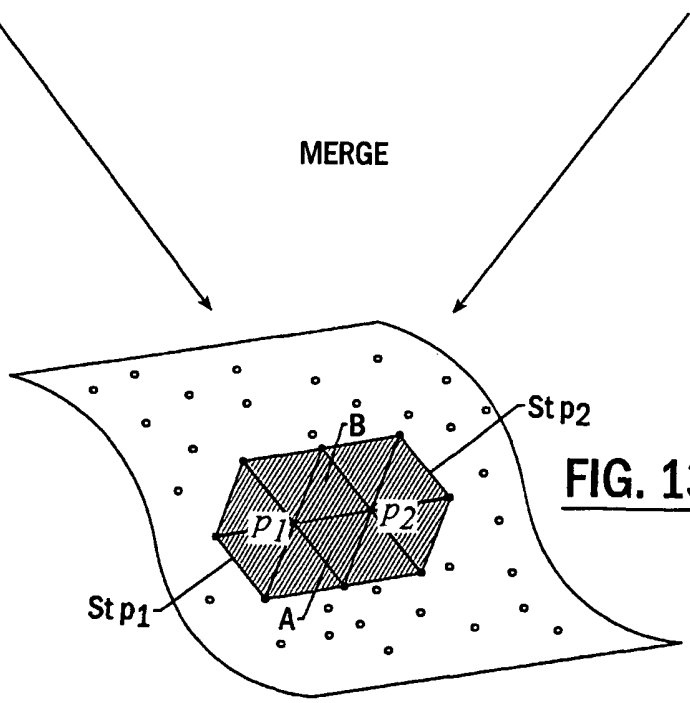

FIG. 13.

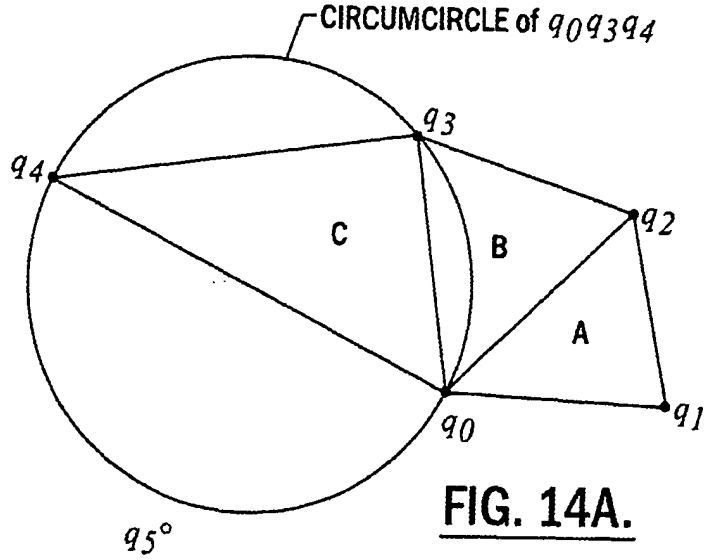

FIG. 14A.

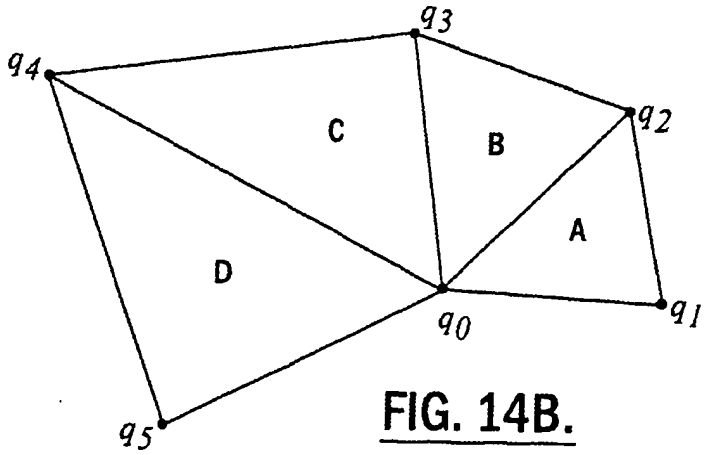

FIG. 14B.

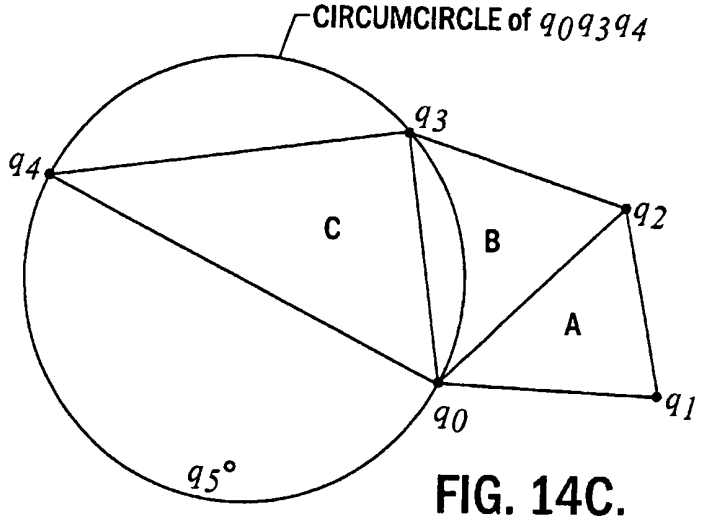

FIG. 14C.

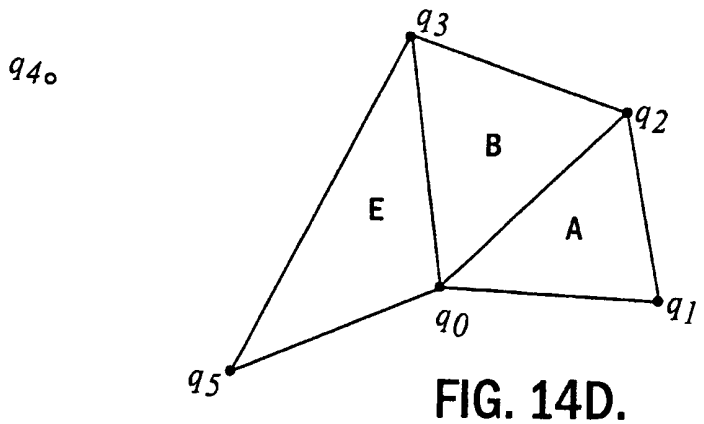

FIG. 14D.

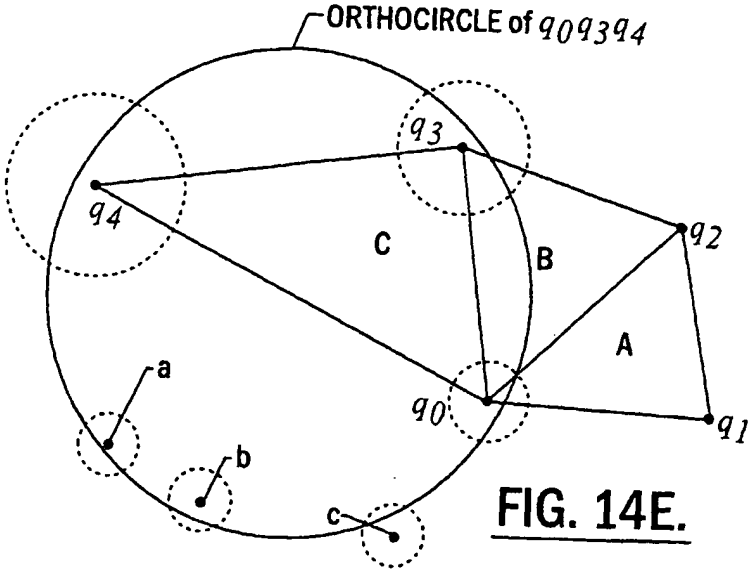

FIG. 14E.

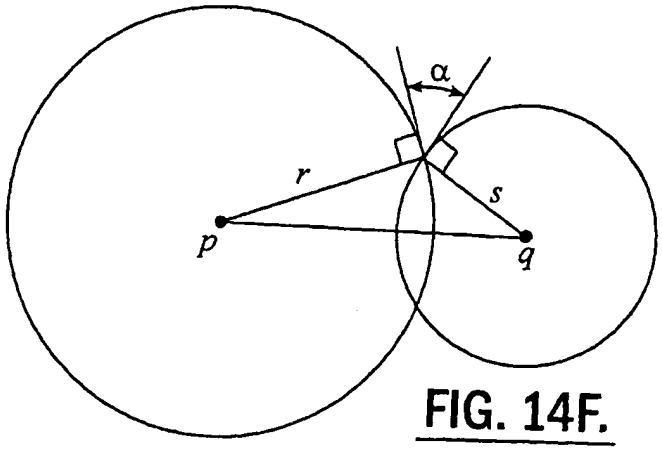

FIG. 14F.

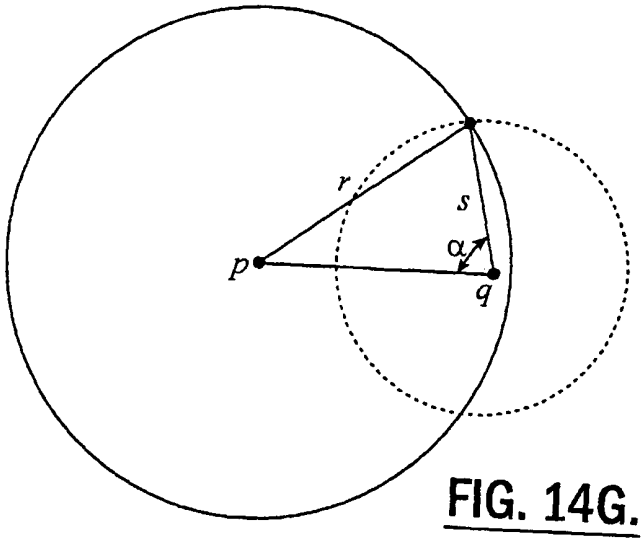

FIG. 14G.

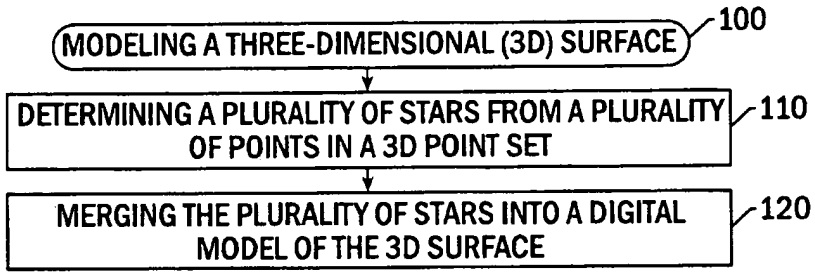
MODELING A THREE-DIMENSIONAL (3D) SURFACE
100
DETERMINING A PLURALITY OF STARS FROM A PLURALITY OF POINTS IN A 3D POINT SET
110
MERGING THE PLURALITY OF STARS INTO A DIGITAL MODEL OF THE 3D SURFACE
120

FIG. 15.

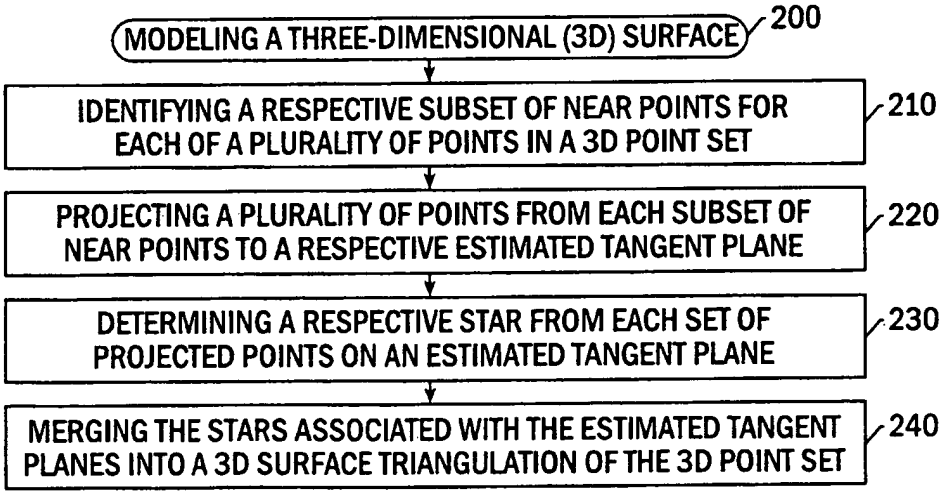
MODELING A THREE-DIMENSIONAL (3D) SURFACE
200
IDENTIFYING A RESPECTIVE SUBSET OF NEAR POINTS FOR EACH OF A PLURALITY OF POINTS IN A 3D POINT SET
210
PROJECTING A PLURALITY OF POINTS FROM EACH SUBSET OF NEAR POINTS TO A RESPECTIVE ESTIMATED TANGENT PLANE
220
DETERMINING A RESPECTIVE STAR FROM EACH SET OF PROJECTED POINTS ON AN ESTIMATED TANGENT PLANE
230
MERGING THE STARS ASSOCIATED WITH THE ESTIMATED TANGENT PLANES INTO A 3D SURFACE TRIANGULATION OF THE 3D POINT SET
240

FIG. 16.

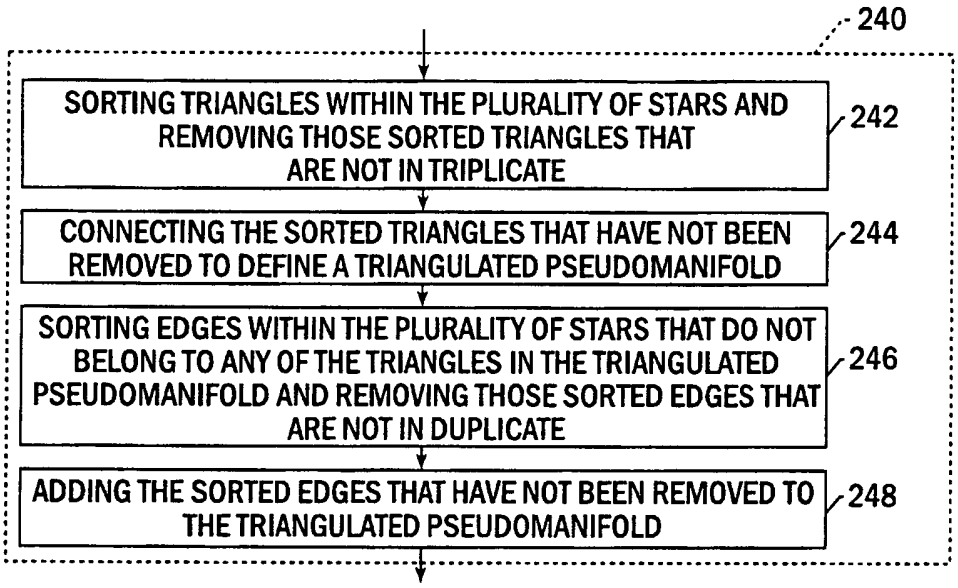
240
SORTING TRIANGLES WITHIN THE PLURALITY OF STARS AND REMOVING THOSE SORTED TRIANGLES THAT ARE NOT IN TRIPLICATE
242
CONNECTING THE SORTED TRIANGLES THAT HAVE NOT BEEN REMOVED TO DEFINE A TRIANGULATED PSEUDOMANIFOLD
244
SORTING EDGES WITHIN THE PLURALITY OF STARS THAT DO NOT BELONG TO ANY OF THE TRIANGLES IN THE TRIANGULATED PSEUDOMANIFOLD AND REMOVING THOSE SORTED EDGES THAT ARE NOT IN DUPLICATE
246
ADDING THE SORTED EDGES THAT HAVE NOT BEEN REMOVED TO THE TRIANGULATED PSEUDOMANIFOLD
248

FIG. 17.

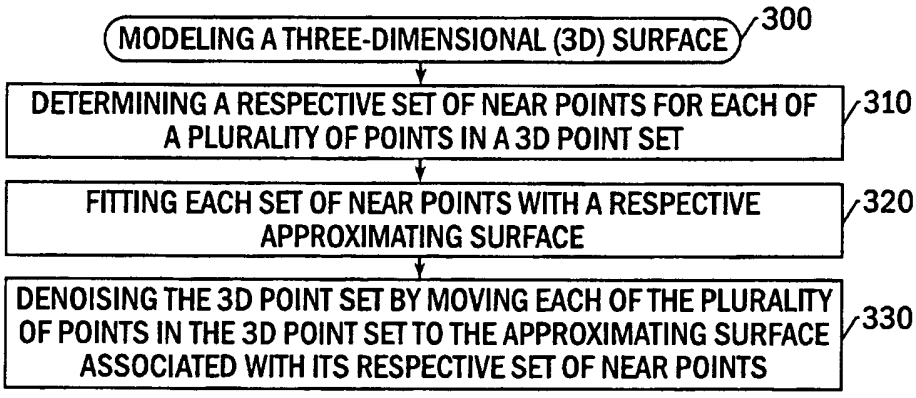
MODELING A THREE-DIMENSIONAL (3D) SURFACE
300
DETERMINING A RESPECTIVE SET OF NEAR POINTS FOR EACH OF A PLURALITY OF POINTS IN A 3D POINT SET
310
FITTING EACH SET OF NEAR POINTS WITH A RESPECTIVE APPROXIMATING SURFACE
320
DENOISING THE 3D POINT SET BY MOVING EACH OF THE PLURALITY OF POINTS IN THE 3D POINT SET TO THE APPROXIMATING SURFACE ASSOCIATED WITH ITS RESPECTIVE SET OF NEAR POINTS
330

FIG. 18.

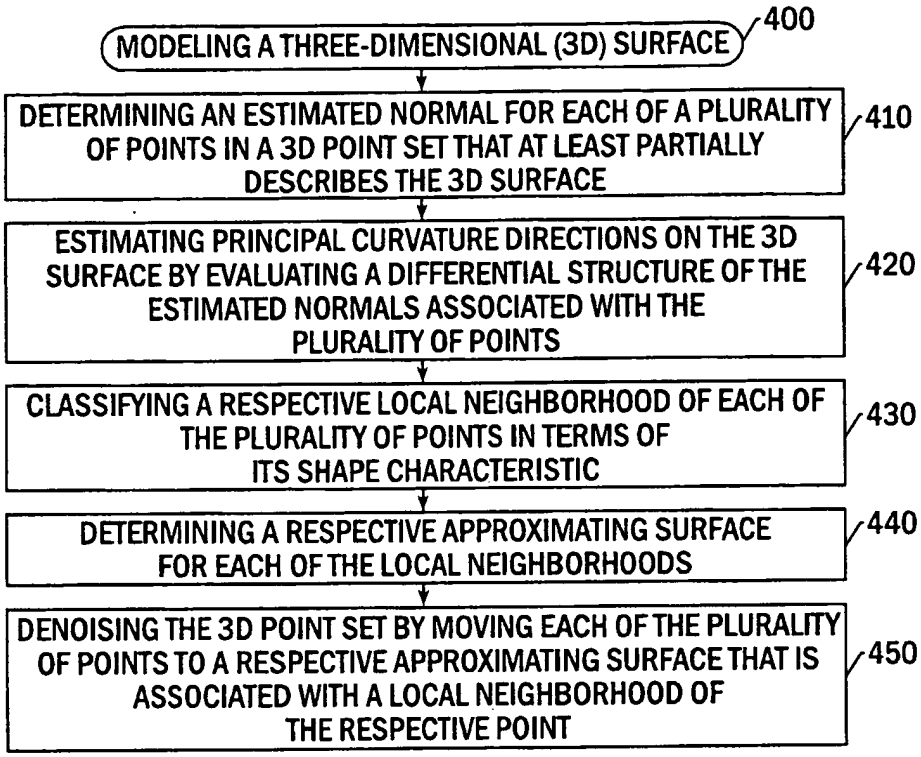
MODELING A THREE-DIMENSIONAL (3D) SURFACE
400
DETERMINING AN ESTIMATED NORMAL FOR EACH OF A PLURALITY OF POINTS IN A 3D POINT SET THAT AT LEAST PARTIALLY DESCRIBES THE 3D SURFACE
410
ESTIMATING PRINCIPAL CURVATURE DIRECTIONS ON THE 3D SURFACE BY EVALUATING A DIFFERENTIAL STRUCTURE OF THE ESTIMATED NORMALS ASSOCIATED WITH THE PLURALITY OF POINTS
420
CLASSIFYING A RESPECTIVE LOCAL NEIGHBORHOOD OF EACH OF THE PLURALITY OF POINTS IN TERMS OF ITS SHAPE CHARACTERISTIC
430
DETERMINING A RESPECTIVE APPROXIMATING SURFACE FOR EACH OF THE LOCAL NEIGHBORHOODS
440
DENOISING THE 3D POINT SET BY MOVING EACH OF THE PLURALITY OF POINTS TO A RESPECTIVE APPROXIMATING SURFACE THAT IS ASSOCIATED WITH A LOCAL NEIGHBORHOOD OF THE RESPECTIVE POINT
450

FIG. 19.

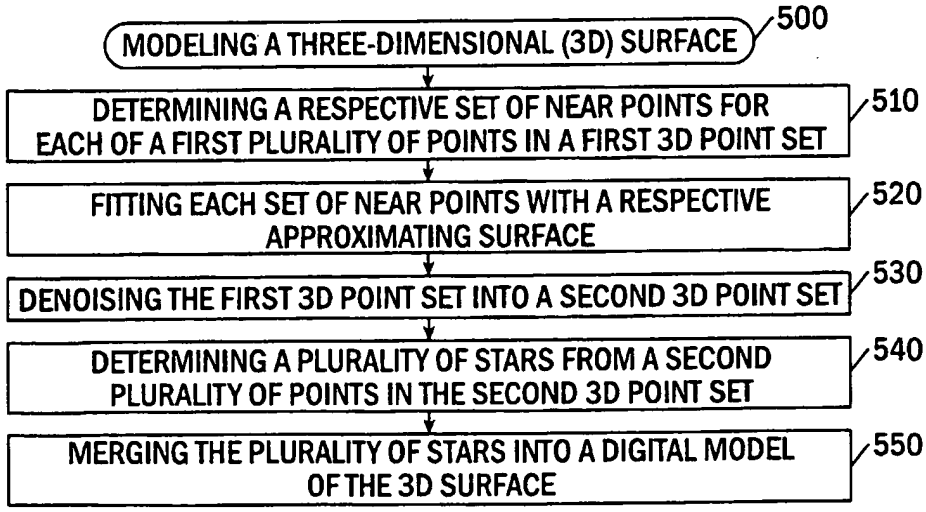
MODELING A THREE-DIMENSIONAL (3D) SURFACE
500
DETERMINING A RESPECTIVE SET OF NEAR POINTS FOR EACH OF A FIRST PLURALITY OF POINTS IN A FIRST 3D POINT SET
510
FITTING EACH SET OF NEAR POINTS WITH A RESPECTIVE APPROXIMATING SURFACE
520
DENOISING THE FIRST 3D POINT SET INTO A SECOND 3D POINT SET
530
DETERMINING A PLURALITY OF STARS FROM A SECOND PLURALITY OF POINTS IN THE SECOND 3D POINT SET
540
MERGING THE PLURALITY OF STARS INTO A DIGITAL MODEL OF THE 3D SURFACE
550

FIG. 20.

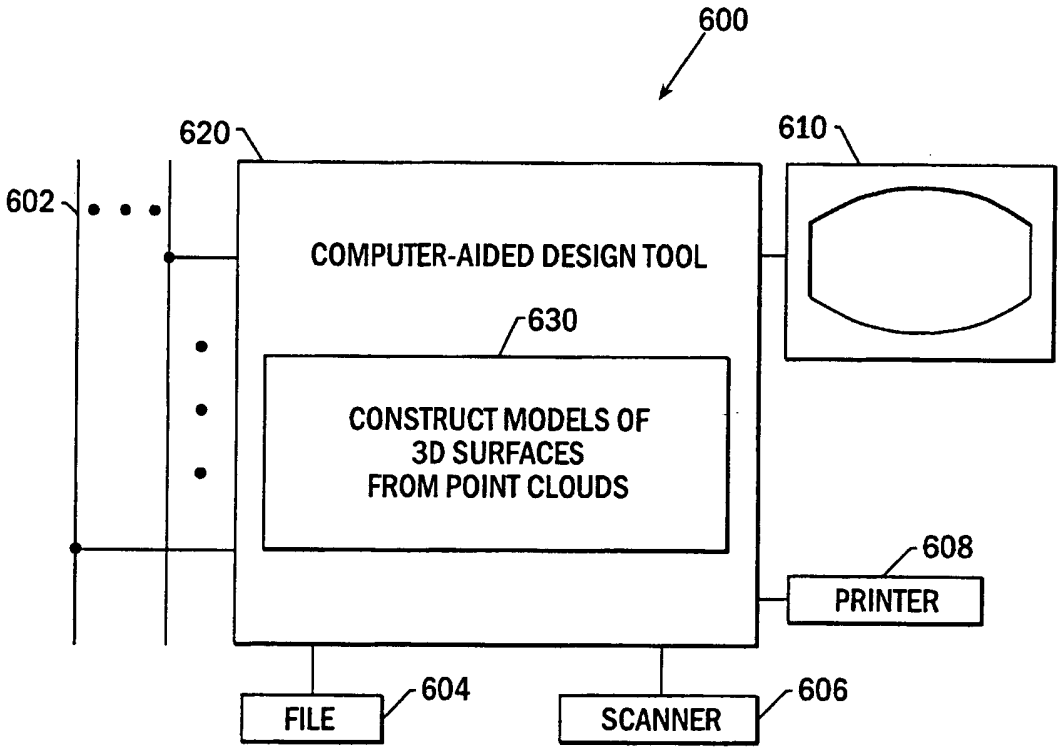
600
620
610
602
COMPUTER-AIDED DESIGN TOOL
630
CONSTRUCT MODELS OF
3D SURFACES
FROM POINT CLOUDS
608
PRINTER
FILE
604
SCANNER
606

FIG. 21.